JGR Planets

REVIEW ARTICLE
10.1029/2022JE007684

Martian Araneiforms: A Review

L. E. Mc Keown[1], S. Diniega[1], G. Portyankina[2], C. J. Hansen[3], K.-M. Aye[4], S. Piqueux[1], and J. E. C. Scully[1]

[1]Jet Propulsion Laboratory, California Institute of Technology, Pasadena, CA, USA, [2]DLR Berlin, Berlin, Germany, [3]Planetary Science Institute, Tucson, AZ, USA, [4]Freie Universtität Berlin, Berlin, Germany

Key Points:

- We review and synthesize the body of literature surrounding the study of Martian araneiforms over the last ~two decades
- We provide discussions on observations made through remote sensing of araneiforms, as well as laboratory analog and numerical modeling work
- We present open questions and offer ways in which they can be addressed to advance the field moving forward

Supporting Information:

Supporting Information may be found in the online version of this article.

Correspondence to:

L. E. Mc Keown,
lauren.mckeown@jpl.nasa.gov

Citation:

Mc Keown, L. E., Diniega, S., Portyankina, G., Hansen, C. J., Aye, K.-M., Piqueux, S., & Scully, J. E. C. (2023). Martian araneiforms: A review. *Journal of Geophysical Research: Planets*, *128*, e2022JE007684. https://doi.org/10.1029/2022JE007684

Received 29 NOV 2022
Accepted 2 MAR 2023

Author Contributions:

Conceptualization: L. E. Mc Keown
Data curation: L. E. Mc Keown
Formal analysis: L. E. Mc Keown, S. Diniega, G. Portyankina, C. J. Hansen, K.-M. Aye, S. Piqueux
Funding acquisition: S. Diniega
Investigation: L. E. Mc Keown, S. Diniega
Methodology: L. E. Mc Keown
Project Administration: S. Diniega
Supervision: S. Diniega

Abstract Araneiforms are enigmatic dendritic negative topography features native to Mars. Found across a variety of substrates and exhibiting a range of scales, morphologies, and activity level, they are hypothesized to form via insolation-induced basal sublimation of seasonal CO_2 ice. With no direct Earth analog, araneiforms are an example of how our understanding of extant surface features can evolve through a multipronged approach using high resolution change-detection imaging, conceptual and numerical modeling, and analog laboratory work. This review offers a primer on the current state of knowledge of Martian araneiforms. We outline the development of their driving conceptual hypothesis and the various methodologies used to study their formation. We furthermore present open questions and identify future laboratory and modeling work and mission objectives that may address these questions. Finally, this review highlights how the study of araneiforms may be used as a proxy for local conditions and perhaps even past seasonal dynamics on Mars. We also reflect on the lessons learnt from studying them and opportunities for comparative planetology that can be harnessed in understanding unusual features on icy worlds that have no Earth analog.

Plain Language Summary Araneiforms, more colloquially coined "spiders," are strange branched networks of troughs that are carved in the Martian regolith within the south polar regions, poleward of ~70°. They have been proposed to form in spring, when sunlight passes through and heats the Martian seasonal CO_2 ice layer, causing gas to build up beneath it and crack the ice, scouring squiggly and branched troughs on the surface and depositing the eroded material in the form of a plume. Such a process does not occur on Earth, so since their original detection, scientists have used creative approaches to understand the formation of araneiforms; comprising computational mathematical modeling, small-scale experiments in planetary chambers to recreate the process, and even citizen science campaigns, where planetary enthusiasts have helped to map their locations on Mars. We review the work that has been conducted to understand the formation of these beautiful and puzzling surface features and discuss how they may help us to understand seasonal change on Mars in the present-day and even the past. We discuss how our understanding of araneiforms can be applied to other icy planetary surfaces and finally present gaps in our knowledge and ways to address them.

1. Introduction

Araneiforms are some of the most intriguing surface expressions found on another planet in that they are active today, have no direct Terrestrial analog, and represent a formation process that is unlike anything seen on Earth. They are defined as converging systems of branching troughs exhibiting fractal properties (G. Portyankina et al., 2020) and comprise a variety of different types based on observed activity and location. These include (a) the original "spiders" (e.g., C. J. Hansen et al., 2010; Piqueux et al., 2003), which are large (up to 1 km in diameter), dendritic, often radial negative topography features restricted to the high south polar latitudes; (b) sand furrows (M. C. Bourke, 2013; M. C. Bourke & Cranford, 2011), which are up to 50 m in length and extend along dune slopes in both hemispheres over a season (then disappearing), and (c) dendritic troughs (G. Portyankina et al., 2019), which have been observed to form and grow interannually on loosely consolidated inter-dune material. All of these features are proposed to be formed by some variant of a "geyser" (non-geothermal) process known as the Kieffer model (Kieffer et al., 2006). This model postulates that insolation penetrating through translucent CO_2 ice during spring yields basal sublimation and produces energetic jets. The process can leave fans and spots of dark albedo fines strewn across the ice surface, having scoured the substrate to form dendritic patterns (Kieffer et al., 2006; Piqueux et al., 2003). Fans and spots are identified in the locales of all of these features in spring (N. Thomas et al., 2010), but only both furrows (M. C. Bourke, 2013) and dendritic troughs (G. Portyankina et al., 2017) have been observed to form today.

Visualization: L. E. Mc Keown
Writing – original draft: L. E. Mc Keown, S. Diniega, G. Portyankina, C. J. Hansen, K.-M. Aye, S. Piqueux
Writing – review & editing: L. E. Mc Keown, S. Diniega, G. Portyankina, C. J. Hansen, K.-M. Aye, S. Piqueux, J. E. C. Scully

The nomenclature regarding each of these features has recently been used interchangeably in the literature and thus would benefit from an update. For the purposes of distinction in this paper, we refer to "araneiform" as an umbrella term for all dendritic features, tied to the hypothesis that they all form through a similar process. However, we note that "araneiform" has previously been applied primarily to spiders in the literature. We draw the distinction in terminology between "spiders" (Figure 1), "dendritic troughs" and "furrows" (Figure 2) based on the former being found on high south polar latitude-layered deposits (SPLD) and surrounds, as well as generally being larger in scale and mostly radial, and the latter two being found on dunes or interdune material. The key distinction between furrows and dendritic troughs is that furrows form each spring on dune slopes and are later erased by wind activity, whereas dendritic troughs persist on interdune material and grow interannually (G. Portyankina et al., 2017). The properties of each of these features are described in Table 1.

Since their first detection with the Mars Orbiter Camera (MOC) onboard Mars Global Surveyor (MGS) (Piqueux et al., 2003), araneiforms have been monitored as a high priority science target. Over the last two decades we have benefited from unprecedented high-resolution change-detection imaging on Mars (McEwen et al., 2007) as the HiRISE instrument onboard the Mars Reconnaissance Orbiter (McEwen, 2007) provides high resolution (50 cm pixel^{-1}), high signal-to-noise color and stereo images at low light levels and high polar latitudes. MRO's ground tracks are closely spaced at the south pole, and so repeat images, with a few days-to-weeks separation, can monitor seasonal surface change, including fan and spot development and trough growth, over short temporal baselines (C. J. Hansen et al., 2010; McEwen et al., 2007). Using the spacecraft's ability to roll off-nadir and generate stereo pairs, we have been able to create Digital Terrain Models (DTMs) to study both the small-scale profiles of the surfaces surrounding araneiforms, as well as their individual negative topographies (C. J. Hansen et al., 2010; Sutton et al., 2022).

Why study araneiforms? Perhaps most significantly, extensive imaging has revealed that the local redistribution of surface material due to frost and wind-driven processes is a dominant activity shaping the surface of Mars today (Diniega et al., 2021; C. J. Hansen et al., 2010; Piqueux & Christensen, 2008a, 2008b). For future mission strategy, particularly at the polar regions, it is essential that we quantify the role of environment on surface change and feedback. Furthermore, little is known about *seasonal* activity during past climates on Mars and a better understanding of seasonally driven landforms in the present can offer a window into this past activity. Araneiforms may serve as useful proxy records of seasonal frost conditions, with activity occurring over annual timescales and, for spiders and dendritic troughs, then integrated over many, many winters.

Furthermore, the range of sizes, morphologies, and activity levels found in araneiforms may provide information about frost and substrate conditions over multiple timescales and terrains. Some araneiforms appear to be active today while others do not, and better understanding the reasons behind this distinction may allow us to use their distinct morphologies and activity/lack thereof as a proxy indicator for present and, by extrapolation, past seasonal and substrate conditions. However, the controls exerted by environmental parameters such as dust, ice thickness, sediment consolidation and ambient atmospheric properties on feature morphology have not yet been quantified. Thus, it remains unclear why certain morphologies are observed in specific locations and often occur in clusters.

Araneiform patterns are reminiscent of patterns of growth and form that are fractal so as to optimally "cover" an area despite a simple pattern (Bunde & Havlin, 1996; Mandelbrot, 1982). Such patterns are widely abundant in nature, for example, Earth river systems in drainage basins (Horton, 1945; Miall, 2013), beach rills (Schorgofer et al., 2004), trees leaf and root systems (Pelletier & Turcotte, 2000), and even respiratory systems and nerve networks in the human body (Horsfield, 1976; Turcotte et al., 1998) (Figure 3). However, the similarity to any of these terrestrial systems is only with respect to appearance. The cryojet process responsible for araneiform formation has no likeness on Earth and thus our understanding cannot rely on field studies of natural terrestrial analogs.

In this review of our current understanding of araneiforms, we see an example of a hypothesis-building and testing process that will become more common within planetary science as we explore more extraterrestrial worlds. Lacking a natural terrestrial analog, the development of a conceptual model for extant processes and intersection of several methodologies to test that theory has been key. As will be described, remote-sensing data analysis, laboratory analog work, numerical modeling and even the help of the general public with citizen-science campaigns have been critical in furthering our understanding of these enigmatic, exotic features.

This paper reviews the advances made to understand araneiform formation in each of these areas. For the context of the environment in which araneiforms form, we start with an overview of two likely environmental controls for araneiform formation: (a) the CO_2 cycle and types of frost found on Mars (Section 1.1) and (b) the substrates

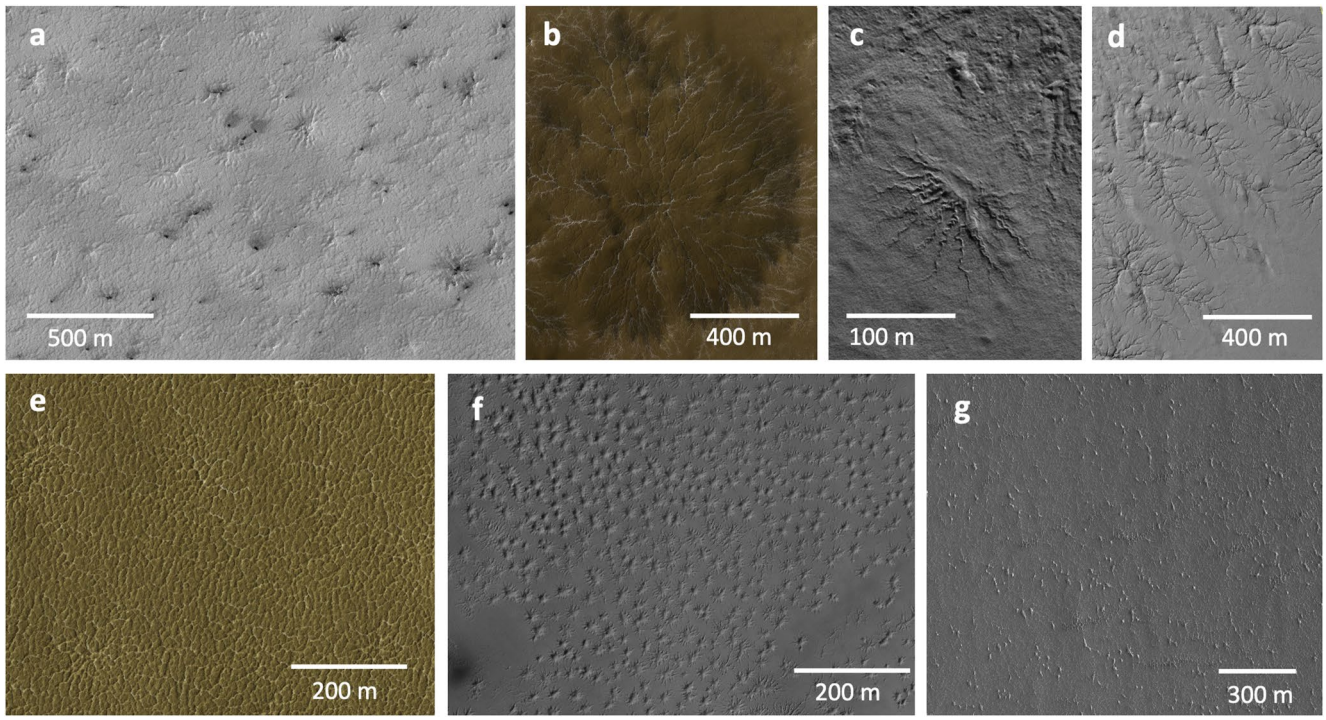

Figure 1. Examples of the many different spider morphologies, previously identified by C. J. Hansen et al. (2010), Hao et al. (2019), Schwamb et al. (2018), and L. Mc Keown et al. (2023b). (a) "Thin" spiders from High Resolution Imaging Science Experiment (HiRISE) image ESP_047991_0980 with central lat = −81.8°N and lon = 302.41°E. (b) "Starburst" spiders in HiRISE color image (to highlight shallow channels) PSP_003443_0980 with central lat = −81.8°N and lon = 76.1°E. (c) "Half" spiders from HiRISE image ESP_013886_0875 with central lat = −87.464°N and lon = 166.109°E, (d) "Linear spiders" in HiRISE image ESP_040664_1050 lat = −74.717°N, lon = 168.412°E. (e) "Lace terrain" in HiRISE color image (to highlight shallow channels) PSP_002532_0935 at lat = −86.4°N and lon = 99.016°E. (f) "Fat spiders" from HiRISE image PSP_005993_0985 with central lat = −81.62°N and lon = 296.39°E. (g) "Baby spiders" in HiRISE image ESP_028998_0935 at lat = −86.315°N and lon = 91.105°E. All images have north facing up, with illumination from the left. Image credit: NASA/JPL/University of Arizona.

found in regions where araneiforms have been identified (Section 1.2). In Section 2, we give an overview of the Kieffer model, which has long been the cardinal hypothesis for araneiform formation. In Section 3, we review jet fan and spot activity observed by remote sensing campaigns. We then focus on the advances made in our understanding of spider (Section 4), furrow (Section 5) and dendritic trough (Section 6) formation via *remote sensing*. Following this, we detail advances in our understanding of araneiforms in general, made through numerical

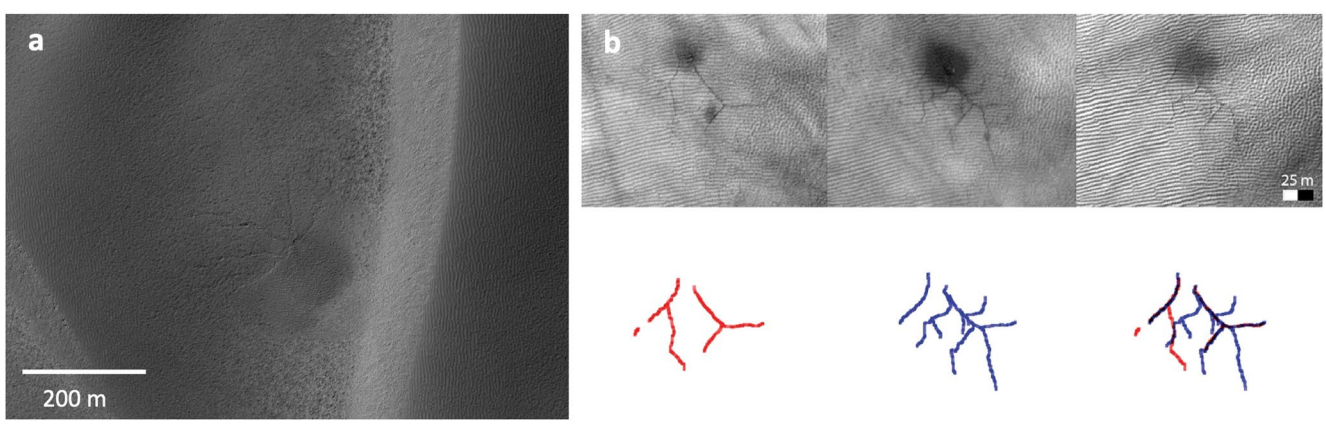

Figure 2. Images of active sand furrows and dendritic troughs. (a) Faint and shallow furrows on sand dunes at latitude −67.608°, longitude 185.343° in the southern hemisphere (High Resolution Imaging Science Experiment (HiRISE) image ESP_023270_1120) form each spring and are later erased by aeolian activity. North is up, illumination is from the left. (b) An example of dendritic troughs enduring and growing on interdune material between 3 Mars Years from MY 29 to MY 32 (G. Portyankina et al., 2017). Images are HiRISE ESP_022255_1095, ESP_031024_1095, ESP_039912_1095, ESP_041402_1095 respectively.

Table 1
Distinct Properties of Three Main Strains of Araneiforms

Feature	Location	Scale	Endurance
Spiders	SPLD/surrounds	<50 m^{-1} km	Perennial
Furrows	>90% dunes in NH, bands in SH	10–100 m	Ephemeral
Dendritic troughs	Interdunes in SH. (Lat, lon = 69.5, 153.4–74.2, 352.2)	<100 m	Growing

Note. NH, Northern Hemisphere; SH, Southern Hemisphere.

modeling (Section 7) and analog laboratory experiments (Section 8). We include a brief discussion on opportunities for comparative planetology (Section 9) and conclude the review with a synthesis of the open questions surrounding araneiforms, and how we may address them going forward in Section 10.

1.1. CO_2 Cycle

The Martian atmosphere is 95% CO_2, which is in vapor equilibrium with the surface (Leighton & Murray, 1966) and contains trace amounts of water vapor (i.e., 0.03% of the atmosphere, or on the order of a few tens of precipitable microns). Annually, both of these volatiles freeze during the cold seasons on Mars, depositing as surface condensate or snowfall (and throughout this paper, we will generally use "frost" to refer to the surface accumulation under either method, including less porous ices that form as the winter progresses). These seasonal frosts are extensive, with the contiguous seasonal frost cap extending out to about 50° latitude (Piqueux et al., 2015) and patchy frost extending down to about 30° latitude (Schmidt et al., 2009). More than a quarter of the CO_2 in the atmosphere condenses into seasonal frost, causing substantial cycling in atmospheric pressure (Forget and Pollack, 1996; Hess et al., 1979; James et al., 1992; Kelly et al., 2006; Leighton & Murray, 1966; Tillman

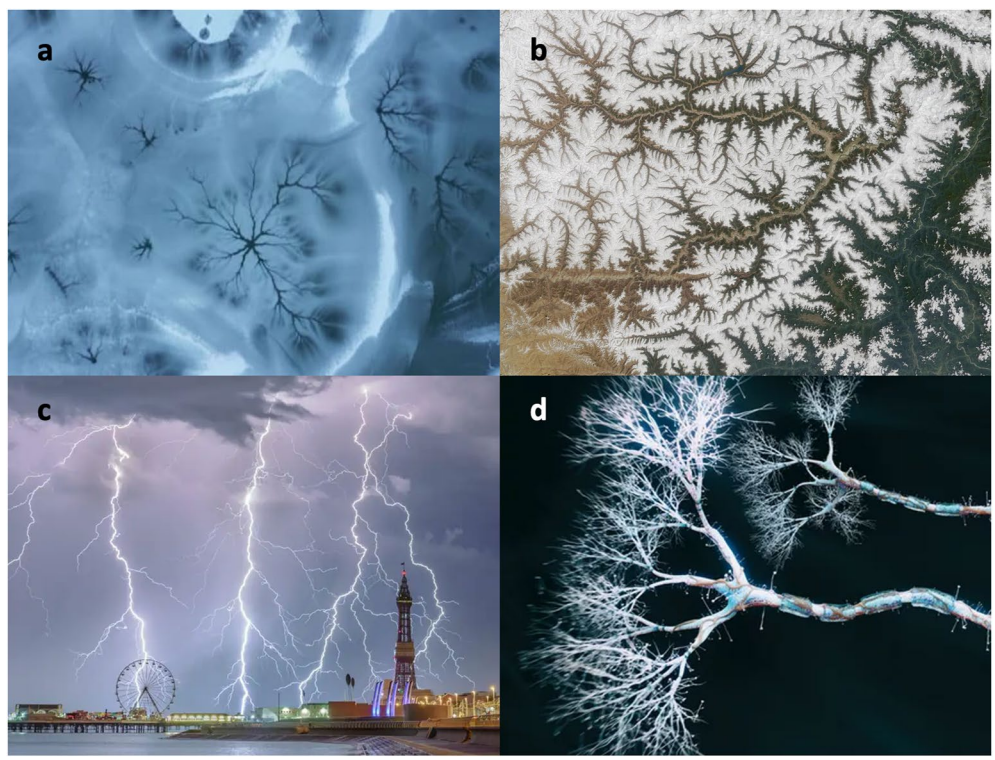

Figure 3. Dendritic Patterns In Nature. (a) Shows "lake stars," which form on Terrestrial lakes in winter. Source: CNN Travel (https://www.cnn.com/travel). (b) Shows drainage patterns in the Yarlung Tsangpo River, Tibet, seen from space. Source: Wikiwand (https://www.wikiwand.com) (c) Shows dendritic lightning strikes. Source: Stephen Cheatley (https://www.bbc.com/news/uk-england-46223996). (d) Depicts artists impression of dendritic patterns in nerve cell endings. Source: iStockphoto.

et al., 1993). The following subsections will describe where and when different frosts form on Mars and the structure of the perennial and seasonal deposits.

Although this paper focuses on CO_2 frost and its geomorphic effects, we acknowledge that it is likely that H_2O and CO_2 frost/ices do not form and evolve independently of each other. Furthermore, their interplay, and interaction with incorporated atmospheric dust, likely constitutes an additional control on geomorphological activity. For example, CO_2 ice can serve as a sink for water vapor (Houben et al., 1997), and H_2O deposits can affect sublimation of porous CO_2 ice (T. N. Titus et al., 2020). Thus, we will briefly describe where and when both H_2O and CO_2 frosts have been detected. However, such interactions are not yet well characterized through observations or models so will not be discussed further within this paper.

1.1.1. The Seasonal Frost Cycle

Seasonal frost on Mars is composed primarily of CO_2, with much lesser amounts of H_2O, due to the planet's atmospheric composition. These frosts condense near 145 and 198 K, respectively, under typical present-day Martian surface conditions (Ingersoll, 1970; James et al., 1992). Orbital daytime observations of CO_2 frost have been observed down to ~42°N (Widmer et al., 2020) and ~33°S (Schorghofer & Edgett, 2006; Vincendon, Mustard, et al., 2010) and minute amounts of nighttime CO_2 frost have been detected from orbit around the equator (Piqueux et al., 2016). Water frost has been observed from orbit at low latitudes (Vincendon, Forget, & Mustard, 2010) and has been observed in situ by rovers near the equator (Landis, 2007; Martínez et al., 2017). As on Earth, the accumulation of frost will depend on latitude, atmospheric conditions such as dust opacity, and local conditions such as shadowing due to topography and surface and subsurface properties (such as grain size and composition, subsurface water ice content and depth) that influence the local thermal inertia (Putzig & Mellon, 2007).

The seasonal cycle stars with a seasonal frost cap forming in the polar regions early in the Martian fall, reaching maximal extent (i.e., equatorward reach) at the end of the fall (Piqueux et al., 2015). Water frost will form first; however, the amount of precipitable water is limited in the tenuous Martian atmosphere, so water frost condensation will depend on the local partial pressure of water vapor and any seasonal water frost accumulations will be very thin (D. E. Smith et al., 2001). In contrast, CO_2 ice requires significantly lower temperatures to condense out of the atmosphere, but is not limited by diffusion through the lower atmosphere due to its much higher abundance. Tens to hundreds of micrometer thick diurnal CO_2 frost layers will form overnight, at lower latitudes as fall and winter progress, eventually extending over a significant fraction of the planet (Piqueux et al., 2016). In addition to the frost that condenses at the surface, CO_2 snowfall contributes to the accumulation in the pole (Gary-Bicas et al., 2020; Hayne et al., 2012, 2014) and midlatitude regions (Widmer et al., 2020).

Accumulated decimeters or thicker layers of seasonal CO_2 frost will sinter, forming polycrystalline CO_2 slab ice(s) (Matsuo & Heki, 2009; Xiao, Stark, Schmidt, Hao, Steinbrügge, et al., 2022; Xiao, Stark, Schmidt, Hao, Su, et al., 2022), with volume densities of up to 1,250 kg/m^3 (Litvak et al., 2007). Seasonal ice sheets reach up to 2 m in thickness near the poles (D. E. Smith et al., 2001; Kelly et al., 2006) and fractured ice layers and detached ice blocks have been observed in the mid-latitudes (Diniega et al., 2013; Dundas et al., 2012; L. E. Mc Keown et al., 2017).

In spring, as the Martian surface warms, the accumulated CO_2 frost/ice will sublime (along with, eventually, the H_2O frost/ice) but not uniformly. CO_2 ice has optical and thermal properties very different from terrestrial water frost and ice, including being transparent to visible wavelengths but opaque to thermal infrared (Kieffer et al., 2000). Via a process known as the solid state greenhouse effect (Matson & Brown, 1989), because it is analogous to the greenhouse effect in planetary atmospheres but happens in a transparent solid body instead of a gaseous atmosphere, visible solar radiation will penetrate the CO_2 ice layer and induce basal sublimation of the impermeable slab ice (Aharonson, 2004; Kieffer et al., 2006). These gases build up until a weakness is found in the ice and the sublimed CO_2 can vent (Pilorget et al., 2011). This venting results in defrosting marks, such as sublimation spots, fans, and dark linear "flow" features (Gardin et al., 2010; Kaufmann & Hagermann, 2017; Kieffer, 2007; Malin & Edgett, 2001; Pilorget et al., 2011, 2013), and polygonal fracturing of the ice slab (Piqueux & Christensen, 2008a, 2008b; G. Portyankina et al., 2012). This seasonal sublimation cycle, described by the Kieffer model (see Section 2), can be very energetic and is thought to be a key driver for the formation of many landforms (Diniega et al., 2021; Pilorget et al., 2011), including araneiforms.

1.1.2. Cryptic Terrain

As the seasonal cap retreats, its appearance is unusual within a swath between 75°S and 85°S latitudes and 50°E and 210°E longitude (Figure 4). This region, named "cryptic terrain" in Kieffer et al. (2000), darkens to resemble

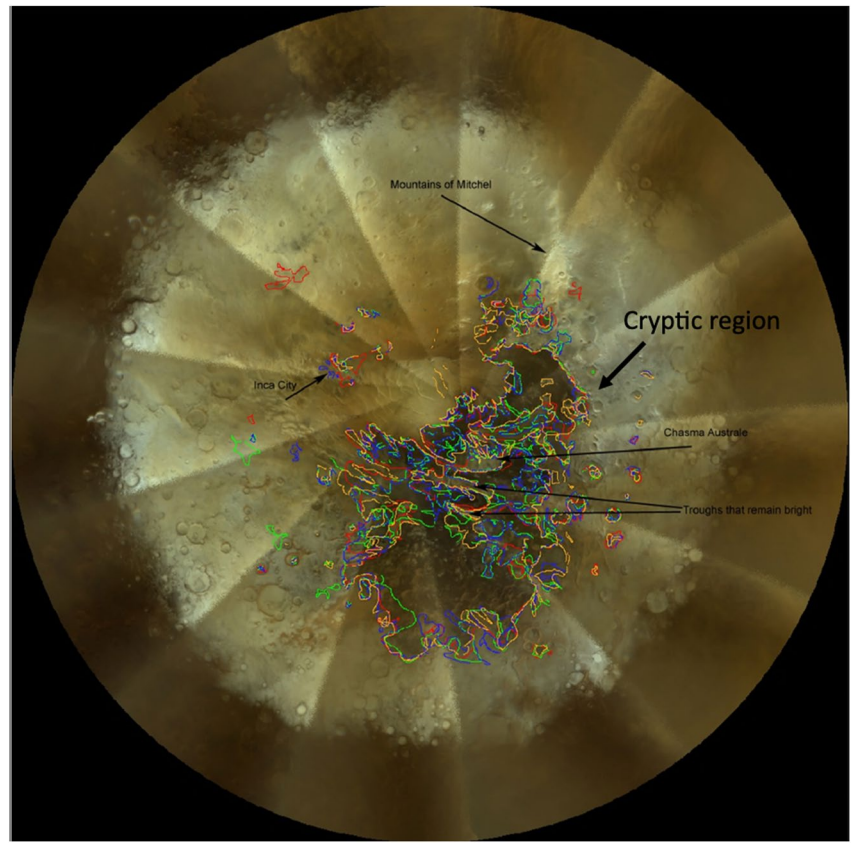

Figure 4. MARCI image of the dark albedo cryptic region of the seasonal CO_2 ice cap. Colors show the outline of the cryptic region; MY 28 is red, MY 29 is green, MY 30 is blue, MY 31 is orange (W. Calvin et al., 2017).

a frost-free substrate but retains a temperature at the CO_2 frost point and so is still covered in ice. Identification of this translucent, early spring ice, along with its spatial correlation with the spiders identified by Piqueux et al. (2003) and extensive fans and other sublimation markers, contributed to the definition of the Kieffer model (Kieffer et al., 2006). The low temperature of this region was first attributed to a clear slab of nearly pure, large grained CO_2 ice, with the low albedo resulting from absorption by the underlying surface. However, Langevin et al. (2006) cited surficial dust as a reason for the dark appearance of the region, showing that modeled spectra of dust contamination in a thin granular layer above a nearly pure layer of CO_2 ice, with the dust very cold due to its close contact, matched the spectral data of Mars Express' OMEGA instrument. Using CRISM spectra over Richardson Crater (180°E, 72°S; along the edge of the cryptic region), Andrieu et al. (2018) found that translucent slab ice is likely present through spring rather than granular ice. The formation of such pure ice slabs was explained by Colaprete et al. (2005) as resulting from differences in atmospheric circulation dynamics leading to differences in CO_2 surface deposition created this distinct feature, with the cryptic region dominated by direct condensation and formation of slab ice rather than snowfall and thus creating larger grained-ice. Schmidt et al. (2010) modeled the sublimated mass around the south pole and found that ~22% more CO_2 accumulates and then sublimes outside the cryptic region, and suggest that this is due to a much higher amount of snowfall in those regions.

Further monitoring of the cryptic terrain has shown that this terrain has a consistent boundary each year, with only small-scale variations (W. Calvin et al., 2017), though there is a dearth of knowledge on how extensive this terrain was in the past or if it appeared at different locations (although it has been observed since 1,845 in telescopic images summarized in T. Titus et al. (2008)). Furthermore, additional small areas have been identified that display similar albedo and temperature, during the spring, as well as gas jet activity resulting in fan-shaped deposits and a similar frost-free surface morphology (W. Calvin et al., 2017; C. J. Hansen et al., 2010). Investigations of elevation and topography have not yielded a clear difference between where cryptic terrain exists and where it is not found (W. Calvin et al., 2017; Xiao, Stark, Schmidt, Hao, Su, et al., 2022; Schmidt et al., 2009), although

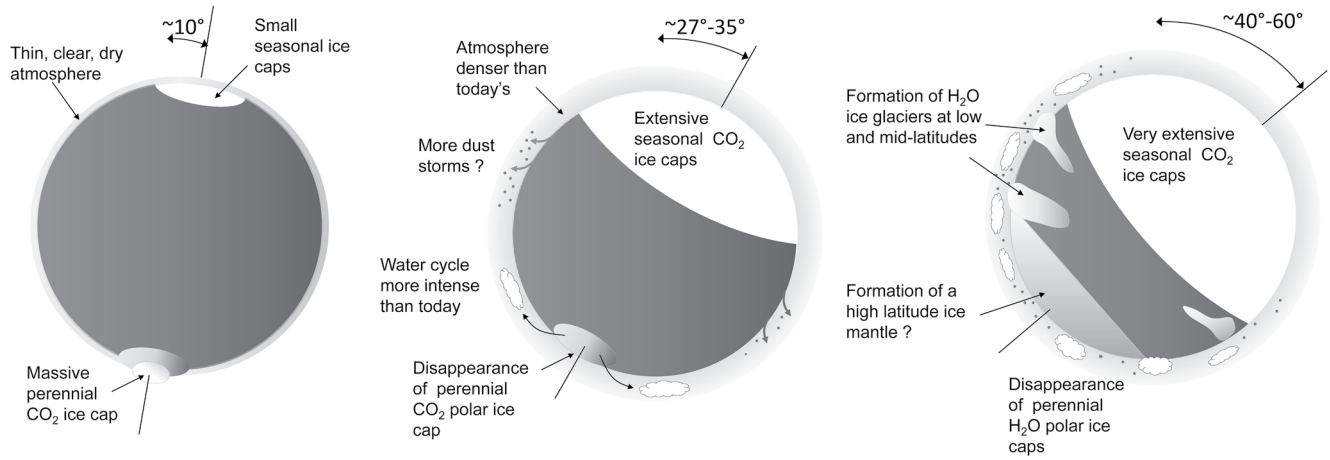

Figure 5. Diagram/cartoon showing seasonal cap extent prediction with obliquity variation. Current Mars obliquity is near the lower amount in the center figure (25°). Source: Forget et al. (2017).

such controls may be mediated through atmospheric dynamics (Colaprete et al., 2005). At present, hypotheses on controls for the annual formation of the cryptic terrain focus on the potential presence of ground ice and how dust within the seasonal frost layer moves around as the seasonal frost evolves through the winter and into spring (W. Calvin et al., 2017; W. M. Calvin & Seelos, 2019).

1.1.3. Frost Accumulation in the Recent Past

In the present Martian climate, seasonal frosts and snowfall events have some interannual variability in terms of location and duration, which have begun to be documented in a systematic manner as more complete records of the present-day climate and weather are acquired (such as W. M. Calvin et al., 2015; Gary-Bicas et al., 2020; Piqueux et al., 2015; Widmer et al., 2020). Over much longer timescales, it is also known that the spatial distribution of seasonal frost deposits and the stability of accumulated seasonal frost/ice will change more substantially due to obliquity and other orbital-parameter changes. For example, models of changing obliquity are used to explain the formation and then ablation or preservation of significant repositories of polar (Bierson et al., 2016; Buhler et al., 2020; Manning et al., 2019) or lower latitude ice (Jakosky et al., 2005; Mellon et al., 1997, 2004). Seasonal cap extent and depth would also change through these cycles, as shown in Figure 5. At present, past climate models are primarily constrained by predictions of planetary obliquity by Laskar and Robutel (1993) and Laskar et al. (2004), which have the Martian obliquity chaotically moving within the range 0°–60°over cycles of tens of thousands to tens of millions of years.

1.2. Properties of the Substrates Where Spiders Are Found

Perennial ices on Mars include the Polar Layered Deposits (PLDs), which extend more than 1,000 km across each pole and are the largest known ice reservoirs on Mars. Radar and gravity data show that both the north and south PLDs (NPLD and SPLD) are composed primarily of H_2O ice with non-ice materials making up a few percent of the total mass (Grima et al., 2009; Plaut et al., 2007; Wieczorek, 2008; Zuber et al., 2007). Similar to polar ice on Earth, the stratigraphy of the PLDs is thought to have formed due to variations in the deposition of ice and dust, reflecting both short-term cycles and long-term climate changes on Mars (Hvidberg et al., 2012; Laskar et al., 2002; Milkovich & Head, 2005; Murray et al., 1972; P. Thomas et al., 1992). The uppermost layer of the PLD of each hemisphere is a residual ice cap (i.e., the North Polar Residual Cap (NPRC) and the South Polar Residual Cap (SPRC)).

As will be discussed in Section 4, spiders have predominantly been identified in the SPLD and have not been observed in the Northern Hemisphere (NH); thus, we focus our description on that pole. Three fundamental types of materials with distinct mechanical or physical properties are present in the SPLD and SPRC:

- Perennial CO_2 ice, forming up to hundreds of meter-thick layered deposits and exposed near the geographical south pole are associated with a wide range of "exotic" sublimation-driven morphologies(P. C. Thomas

et al., 2000), such as swiss cheese (Byrne & Ingersoll, 2003). However, spider-like features have not been observed on these terrains. This absence has generally been interpreted as the consequence of both their high albedo and potential elevated competence compared to nearby terrains, rendering these units especially reflective to solar energy and also not conducive to scouring. More recently, Gary-Bicas et al. (2020), Hayne et al. (2014), Colaprete et al. (2005) have reported unique seasonal CO_2 ice properties above the perennial CO_2 ice, that they linked to enhanced snow fall precipitations during the polar night. These deposits are associated with brighter and opaque seasonal CO_2 ice, and may therefore not be conducive to the basal sublimation found in other portions of the cap. If this is the case, the absence of spider features on exposed perennial CO_2 ice may not just be caused by the intrinsic substrate properties, but also by the optical properties of the overlying seasonal CO_2 ice.

- Water ice, both exposed (Bibring et al., 2004; Piqueux et al., 2008; T. Titus et al., 2003) or found at depths of a few cm to meters (Bandfield & Feldman, 2008; Piqueux et al., 2019), interpreted as massive and nearly pure deposits whose origin varies as a function of unit and hemisphere (Bramson et al., 2017; Morgan et al., 2021; Schorghofer & Forget, 2012). Water ice deposits are generally associated with high thermal inertia values and are associated with patterned ground (e.g., Balme et al., 2013; Séjourné et al., 2011, 2012; Soare et al., 2021). Both attributes point to rock-like competent material properties, potentially not conducive to surficial scouring and the formation of spiders. Nonetheless, the depths of the depressions associated with spiders generally penetrate deeper than the estimated top of the water ice table, suggesting that the formation mechanism of channels is sufficiently powerful to erode massive ice (Piqueux & Christensen, 2008a, 2008b), or, alternatively, that summer-time sublimation of surficial perennial water ice recently exposed by venting is efficient at prepping the regolith for subsequent erosion. Perennial water ice exposed at the north perennial cap also displays high apparent thermal inertia values consistent with porosity gradients with depth (Bapst et al., 2019). The lateral variability of the depth to the water ice table at various lateral length scales (from cm to hundreds of km, see Piqueux et al. (2019)) is vastly unknown and a topic of debate. In the NH, shallow water ice, that is, potentially strongly indurated substrate, is generally found at shallower depths than in the south (Morgan et al., 2021). This difference explains part of the differential behavior between the seasonal caps in terms of extent and timing of growth/retreat and might also be a factor controlling the strong hemispherical dissymmetry between the nature and distribution of araneiforms.
- Fines, forming the vast majority of the surficial material at high latitudes, comprise a 0–1 m thick deposit on top of massive ice. The physical properties of the Martian fines are generally derived from thermal observations, but such retrievals are very difficult in the polar regions due to the absence of well-expressed diurnal cycles and forcings necessary for thermophysical characterization. Generally, the dry surficial regolith has been characterized with thermal inertia values of 200–400 J m^{-2} K^{-1} $s^{-1/2}$ or more in the North, and <200 J m^{-2} K^{-1} $s^{-1/2}$ in the South (Putzig et al., 2005). Respectively, this suggests the presence of coarse sand-like (or coarser) material that is potentially indurated in the North and dust-like, looser material in the South (Paige & Keegan, 1994; Paige et al., 1994; Putzig et al., 2005). Ground-truthing was acquired at the Phoenix landing site, where the thickness of the loose mobile particulated deposit was observed to range from 5 to 18 cm, with a thermal inertia of 250–300 J m^{-2} K^{-1} $s^{-1/2}$, and with an underlying substrate of competent pore ice that was difficult to sample, probably interfacing with massive ice (P. H. Smith et al., 2009; Zent et al., 2010). Unique to the northern high latitudes, a vast polar erg made of loose sand dunes (Diniega et al., 2019; Khuller et al., 2021), possibly indurated in places by water ice (Mellon & Jakosky, 1993, 1995; Putzig et al., 2014), is consistent with thermal data.

As mentioned in Section 1.1.1 and will be described in Section 2, thermal models have shown that sufficient heating is delivered to the base of the CO_2 ice slab so that a pressurized gas layer develops between the ice and the underlying ground. This leads to dust and gas ejection and the formation of defrosting marks (Aharonson, 2004; Gardin et al., 2010; Kaufmann & Hagermann, 2017; Kieffer, 2007; Malin & Edgett, 2001; Pilorget et al., 2011, 2013) and may cause scouring of sandy surfaces, forming araneiforms (G. Portyankina et al., 2017).

Exposed or shallow water ice mixed with fines also forms geologic units with properties recognized to be conducive to the formation of spiders and venting features. Patterned grounds (most often in the form of "polygons") are ubiquitous at mid and high latitudes (Mangold, 2005) in both hemispheres, and are recognized to form as a response to thermal cycling in a water-ice rich subsurface material (Mellon, 1997). Annually, after the last seasonal ice removal, the Martian surface experiences seasonal temperature variations in excess of 100 K over a very short period of time (Piqueux et al., 2015). The formation of vertical cracks in the ice-rich regolith enables

vertical material sorting (i.e., fines filling up the cracks) and increased preferential sublimation along these fractures (Marchant et al., 2002), but this process would eventually shut down as sufficiently enlarged troughs will remain ice-covered slightly longer than nearby flat terrains. When this occurs on Earth, water ice is retained in the troughs and mixed with the fines. On Mars, this preferential retention of seasonal ice has also been observed on Martian polygons (Mangold, 2005), although CO_2 ice is the likely involved volatile.

Spiders and patterned ground seem intimately related in numerous locations, which has led Piqueux et al. (2008) to suggest that positive feedback may be linking the formation process of both features in some places:

- The development of <100 m dark incomplete polygonal patterns on the seasonal CO_2 ice (in both hemispheres) and the diffuse fan-like darkening of the surface associated with cracks has been interpreted as signs of the venting of dust-rich CO_2 gas from beneath the ice. This is a similar process as the formation of the spiders and blotches (as will be described in Section 3), but with gas ejection along long fracture planes as opposed to point locations. These dark (relative to the surrounding bright seasonal ice) polygons disappear when the seasonal CO_2 ice is gone, as opposed to polygonal pattern grounds, also described as "etched polygons," observed on the bare ground later in the later summer.
- Etched polygons generally form a network of irregularly shaped intertwined meter deep (or more) troughs (at the scale of meters) occasionally associated with typical well-formed spiders (Piqueux et al., 2008) (as will be defined in Section 4.2). These polygons have been proposed to result from the horizontal migration of CO_2 gas after sublimation at the interface of the regolith and seasonal CO_2 ice along preferential gas flow paths developed and maintained spring after spring (Piqueux et al., 2008). Aeolian fines filling the wedges of common high latitude Martian polygons may provide a medium conducive to efficient CO_2 gas flow and clast entrainment at the time of basal sublimation, further suggesting that common high latitude polygons may behave as precursors to etched polygons. Through a positive feedback loop, those etched polygons may favor the subsequent migration of CO_2 gas, thus favoring again the formation of subsequent dark polygons on the CO_2 cap the following spring.

This model of the interrelated formation mechanism between ground patterns, seasonal dark polygons on the CO_2 ice, and etched polygons on the ice-cemented regolith illustrates the interrelationship between the various seasonal and perennial features unique to the Martin high latitude and the potential control of the substrate mechanical properties on polar processes.

2. The Kieffer Model

At the turn of the millennium, the MOC on MGS detected wide-spread wind streaks (that later would be renamed "fans") on both the northern and southern seasonal caps (Malin & Edgett, 2001). Bright streaks were mainly thought to be composed of frost, and dark streaks of sediment material. In the same areas, a whole "zoo" of surface phenomena were identified within observations by TES, THEMIS, and MOC, with informal but descriptive names such as cryptic material, Dalmatian spots, oriented fans, black spiders, and fried eggs (Kieffer, 2003). None of these features had any likeness on Earth, and thus, a conceptual model was needed in the absence of field analogs.

Some other formation hypotheses were offered, including a brine-melt hypothesis (Prieto-Ballesteros et al., 2006); however, the driving conceptual formation model was suggested by Kieffer to perhaps be related to CO_2-gas based jet eruptions (first mentioned in Kieffer (2000)) through the seasonal CO_2 frost (Kieffer et al., 2006) (Figure 6). The full model, described in Kieffer et al. (2006) and Kieffer (2007) and generally referred to as *the Kieffer model*, was the first comprehensive description of the process creating the hypothesized jets that were thought to be responsible for the observed wind streaks and other features, including spiders (Piqueux et al., 2003), and has been well-accepted by the community for the last two decades.

Inspired by the initial model proposed to explain the dark plumes of Triton (Brown et al., 1990; Kirk et al., 1990; Soderblom et al., 1990; B. A. Smith et al., 1989), Kieffer et al. (2006) postulated that the Martian jets occurred due to basal sublimation driven by a Solid State Greenhouse Effect (Matson & Brown, 1989). There are several important components which we delineate below for the purpose of this review, as each step has motivated later key supporting remote-sensing and laboratory/numerical modeling work (further described in sections and 7 and 8).

1. **Condensation of CO_2 Slab Ice:** The physical properties of the CO_2 ice that overlies araneiforms form an essential tenet of Kieffer's model. That is, the ice observed in the cryptic region and concurrent with "cryptic material" takes the form of impermeable *slab ice.* This polycrystalline ice form of CO_2 has the distinct properties of being translucent in the visible and opaque in the thermal infrared wavelength ranges (G. B.

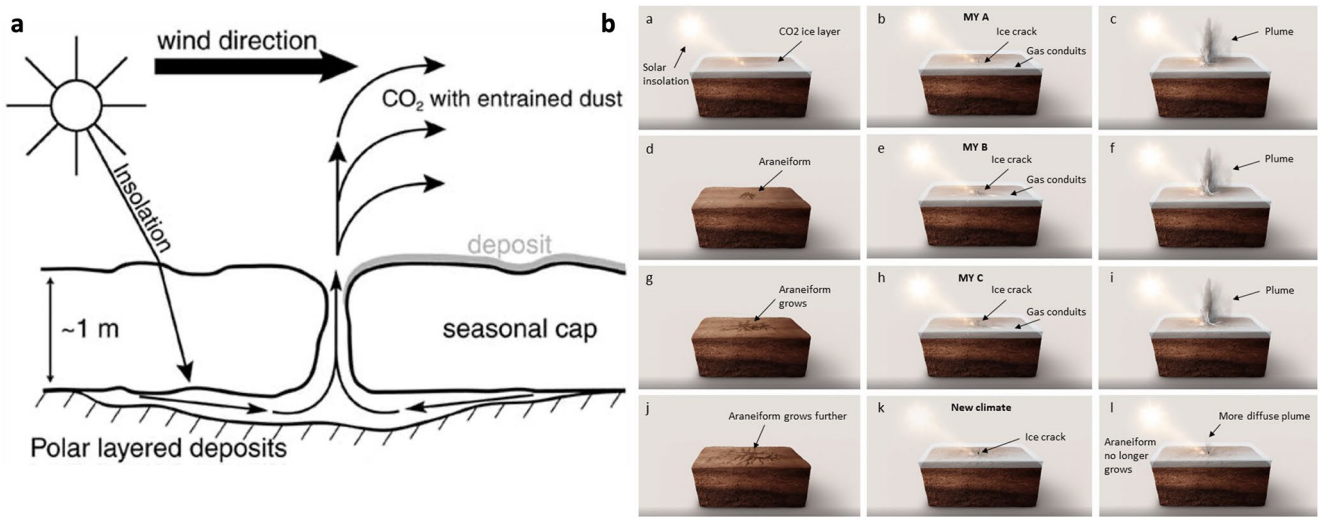

Figure 6. (a) Original sketch of the Kieffer model (Piqueux et al., 2003). (b) Sketch showing potential stages of spider growth over subsequent sublimation episodes, suggesting that some spiders may have developed in few instances during past climatic conditions. These images show a "cut-out" of Martian terrain with the Kieffer model occurring during subsequent Mars years. From MY A-C, the gas activity forms and grows a spider. During the new climate, this activity is less effective at eroding the substrate (L. Mc Keown et al., 2021). Source: Wax Visuals (https://waxvisuals.com/).

Hansen, 1997). In considering the refraction of sunlight into the ice slab, it was calculated that for average polar summer conditions, ~60% of the solar energy can penetrate 1 m into pure and solid CO_2 and the top 2 mm are in net radiative loss (G. B. Hansen, 1997).

2. **Dust-Ingrained Ice:** Since Mars's atmosphere is dusty, and hence seasonal ice will be dust-ingrained, this poses a quandary for the requirement that incoming sunlight passes through its base. Kieffer posited that dust particulates would act as nuclei upon which atmospheric volatiles could condense in winter. Dust will shorten solar absorption lengths, causing net radiation loss at the surface of the dusty ice. Combined with enhanced solar flux at the top layer of the slab, the uppermost layer of the ice is proposed to be clean, with a concentration of dust in the lower material (Kieffer, 2003).
3. **Self-Cleaning:** *Within* the ice, incoming radiation is absorbed in a process known as *self cleaning* (Kieffer, 2003; G. Portyankina et al., 2010). Because the CO_2 surrounding the dust grains is isothermal, the radiation absorbed by the grains will cause the CO_2 local to each grain to sublimate. If the CO_2 is impermeable, this sublimation will generate a high pressure "vapor prison" surrounding the dust grains, analogous to that observed for dancing water droplets on a hot pan in a phenomenon known as the Leidenfrost Effect (Leidenfrost, 1966). If the cushion of gas surrounding the dust grain does not burst and if the dust grain rests at the bottom of the bubble, vapor will re-condense on the surface of the vapor prison where it is coolest, ultimately weighing on the bubble and driving the dust grain downwards as it continues to cause its surroundings to sublimate. The trail will leave a sealed vertical "column' which will travel down with the grain until it reaches the bottom of the ice where it is expelled onto the regolith beneath.
4. **Annealing:** Following deposition, fine-grained CO_2 ice can undergo annealing (?) and metamorphose into impermeable slab ice. Incoming solar radiation can now penetrate the translucent ice layer to the depth of its base, heating the optically opaque regolith beneath and in turn, causing the ice above it to sublimate. The net positive radiation divergence at the surface of the ice layer is posited to seal the gaps in the ice formed by this self-cleaning process. Annealing of the ice is key because it causes the ice to be non-porous, meaning that basal sublimation gas formed by insolation penetrating the ice generally cannot diffuse upward.
5. **The Formation of Vents:** Gas formed through basal sublimation is trapped, reaching, in some cases, a pressure several times the atmospheric pressure (Kieffer, 2003). The gas must escape somewhere to a region of lower pressure, and thus as pressure builds, the ice will crack, forming vents through which the gas will escape. Gas will also travel laterally to the edge of the deposit. Kieffer calculated, based on ice properties and insolation receipt, that the total spacing of the vents must collectively carry a total sublimation gas flux of 10 kg m^{-2} per day. G. Portyankina et al. (2010) showed that these outbursts happen very early in spring.
6. **Araneiform Formation:** Thermal inertia measurements of the cryptic region are low, indicating that loosely consolidated regolith is present in this region. If the effective vents are spaced further apart than the ice is

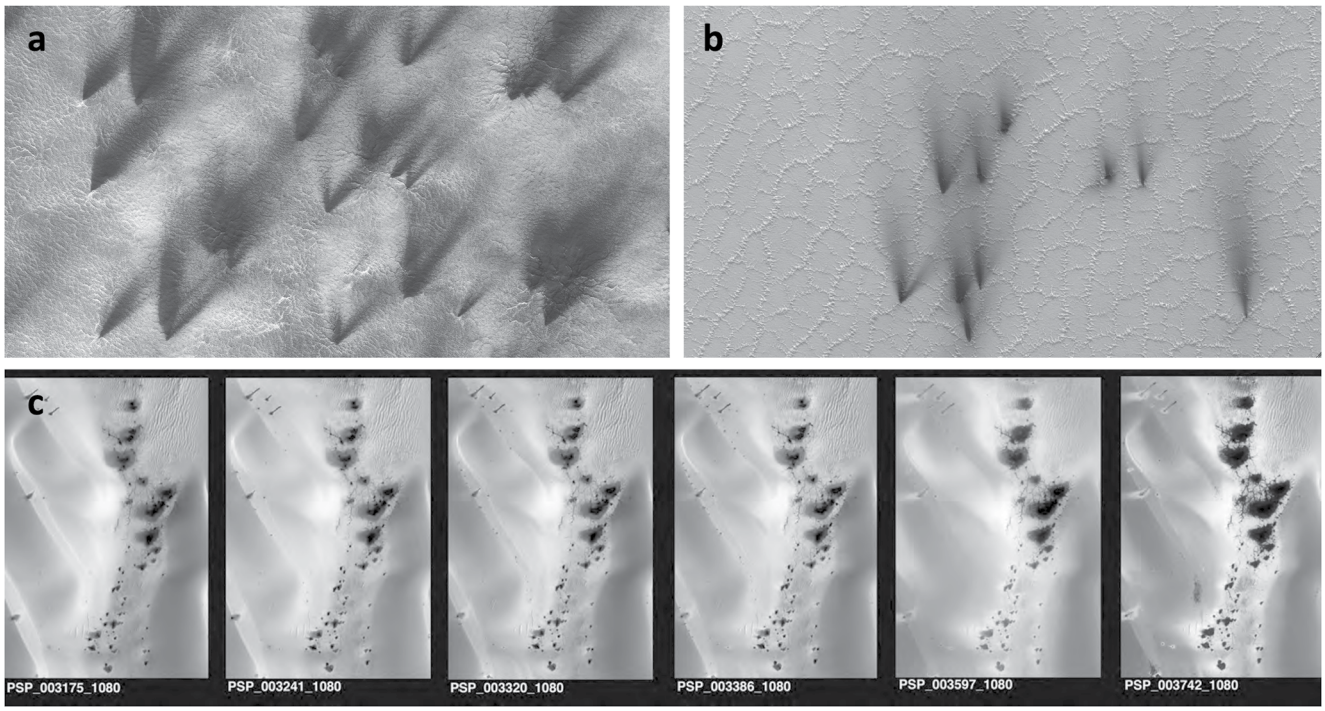

Figure 7. (a) Set of fans with multiple orientations, indicating that multiple eruptions occurred under changed wind directions. Because each set of fans are well aligned with each other, a simultaneous eruption event from multiple vents with contemporaneous ejection of substrate material is more likely than delayed ground redistribution of material by winds from a jet-induced ground exposure. Image source: High Resolution Imaging Science Experiment (HiRISE) ID PSP_003180_0945. (b) Fans emanating from within the troughs of etched polygons. Image source: HiRISE ID ESP_011348_0950. (c) A series of HiRISE images (PSP_003175_1080, PSP_003241_1080, PSP_003320_1080, PSP_003386_1080, PSP_003597_1080, PSP_003742_1080) of the evolution of "fried eggs" from earlier presentations of "Polar Pictionary" by Hansen, with reference to the "Zoo" of features described by Kieffer (2003).

thick (Kieffer, 2003), gas velocities will exceed the fluid threshold (Greeley et al., 1992) and loose material can be suspended and erosion of the substrate can begin. The flow may also diffuse through the regolith. The high velocity gas (on the order of >10 m s^{-1} for saltation (Greeley et al., 1992; Zurek et al., 1992)) will travel toward the vent, entraining particulate material in its wake to scour the surface and erode the dendritic patterns that characterize araneiforms. Gas velocity will depend on the flow geometry (N. Thomas et al., 2011b), but the presence of dust particles in the flow might instigate motion and scouring can occur at lower velocities Kieffer (2003), with velocity building toward the vent and hence increasingly large particles can be lifted here. As with many instability-driven systems (Saffman & Taylor, 1958), the circularly symmetric flow of gas toward the vent is unstable and thus dendritic patterns develop. Kieffer credited this process as responsible for the significant central pit connected to dendritic radial channels of what the MOC team originally dubbed "black spiders." It was noted as early as this model was developed that the velocity in the vents is proportional with the square of the ratio of vent separation to vent diameter.

7. **Fans/Spot Formation and Plume Activity:** After the surface material has been eroded and entrained within the flow, velocities will have built to expel the regolith in the form of a plume. As this jet energy drains, the relatively dark albedo material will be deposited onto the ice surface, often in a circular shape surrounding the vent, known as *spots* or "Dalmatian Spots." Some spots have dark "haloes" which were dubbed "fried eggs" (Figure 7c). Often these spots will coalesce, forming *blotches.* Jets that erupt into an ambient wind will carry particulates and orient the dark material in its prevailing direction to form *fans* (Figures 7a and 7b). Although such activity is ubiquitous within araneiform locations in southern spring, fans and spots are detected in regions where there are no araneiforms.

3. Intriguing Active Icy Features: Jets, Fans and Spots

In the overview of TES results for the south pole of Mars by Kieffer et al. (2000), the "cryptic region" showed an increased appearance of exotic features (as described in Section 1.1.2). In particular, the wind streaks identified

by Malin and Edgett (2001) and Cantor et al. (2002) were observed to mostly occur in this region, despite a global survey. After renaming the streaks as "fans" in Kieffer (2000), Kieffer et al. (2006) fully redefined these surface deposits: some were called "fans," due to their fan-like or ice-cone-like shape, and some were called "blotches" for their roundish to oval shape, still radially symmetric. The latter were assumed to have formed by gas jet eruptions during times with no winds, while the fans aligned with the dominant wind direction at the time of the eruption (Kieffer et al., 2006) (Figure 7a).

While Kieffer's model (see Section 2) ascribes the energy source for the CO_2 sublimation as stemming directly from the insolation penetrating through a highly translucent seasonal CO_2 ice layer, Aharonson et al. (2004) suggested that thermal energy in the ground, deposited during summer and released during the polar night and spring, could induce the sublimation activity. However, Piqueux et al. (2003) countered that the jet activity and hypothesized related araneiform creation seemed to be confined to the cryptic region, while stored thermal energy from the summer should be released from all surfaces around the pole.

With the advent of the HiRISE camera at Mars, C. J. Hansen et al. (2010), N. Thomas et al. (2010), and G. Portyankina et al. (2010) produced reviews of the spatial distribution and localized variability of sublimation-driven features in the highest available resolution of 50 cm pixel^{-1}. On smaller scales, many of the fans within an area were found to point in the same direction, suggesting that they formed under similar wind conditions and perhaps contemporaneously. Some regions of interest had fans pointing in the same and more than one distinct set of directions, clearly indicating that multiple eruptions had occurred through a change in wind direction (see Figure 7).

Observations like these became possible with so-called "seasonal campaigns" of the HiRISE instrument, where overlapping images were taken over a region so as to track changes in the appearance of frost from the spring to summer, when the surface would become ice-free. It is notable that the HiRISE camera is so sensitive that it became possible to perform imaging with only indirect sunlight reflected from the atmosphere before the beginning of polar spring (i.e., as early as L_s, or solar longitude, 173).

N. Thomas et al. (2010) showed that even at these very early times, with only a very small amount of indirect insolation, fan-shaped surface deposits could be observed at high latitudes, specifically in the region called "Inca City" (81.68°S and 296.75°E). It is believed that the local surface inclinations in that area collect more of the sparse, indirect sunlight, inducing this earliest activity, and simulations of breaking the seasonal ice in G. Portyankina et al. (2010) indicate that eruption events were indeed possible and even likely at such an early time after the polar winter. To this day, the exact shapes and color developments of fans and blotches, and the inexplicably sharp divides between active and inactive areas remain a focus of new studies, including those using newer cameras such as the CaSSIS instrument on the European Trace Gas Orbiter (TGO, Cesar et al., 2022).

Since the fans are thought to record wind directions at the time of the jet eruption, systematically mapping the fans would yield a broad-scale, high spatial resolution map of polar winds (at least during certain portions of the polar winter). However, early attempts at such a mapping, such as that by Aye et al. (2010), required a manual step of determining the best thresholding value for determining dark pixels under variable contrast conditions over the spring and summer images. Around the same time, experiments started with having some kind of computerized outlining system, either on a website or by specialized applications, to create a catalog of identified fans and their directions. However, the technology stack required to do this on a bigger scale was cumbersome in those days and the effort to teach users how to use it and to obtain the data for analysis and reduction was high. Things changed with the appearance of the Zooniverse platform (Lintott et al., 2010), a web-based citizen science visual analysis framework. The fan-marking project "Planet Four" aimed to geometrically combine markings of dozens of volunteers into reliable shapes and directions of fans and blotches, and eventually a catalog of several hundred thousands of surface located objects were produced, including all data required to redraw their shape on given geographical coordinates (Aye et al., 2019).

4. Spiders

4.1. The Discovery of Spiders on Mars

"Spiders" were first detected by the MOC onboard MGS Malin and Edgett (2001). According to Piqueux et al. (2003), the term "black spiders" was originally coined by Andy Ingersoll and later published by Kieffer (2000), citing them as "dark radially converging dendritic patterns…visible in MOC Narrow Angle (NA) images of some portions of the spring polar cap." From the first studies, these features appeared to be restricted

to the high southern latitudes among the South PLDs (SPLD), where there should be a layer of cemented water ice and soil about 5–10 cm below the surface Mellon et al. (2004), Prettyman et al. (2004) overlain by loosely consolidated granular surface material Boynton et al. (2002), T. Titus et al. (2003), Vasavada et al. (2000).

Spiders were first formally defined and described by Piqueux et al. (2003), with a survey of over 5,000 MOC images polewards of 70° to map them against the cryptic region. Through this comparison, the study aimed to test the early version of the Kieffer Model (Section 2). This study found that the features seemed to be restricted to the SPLD and were not detected on the southern highlands or residual cap. Further study by G. V. Portyankina (2005) extended the survey of spiders to longitudes 10°–120° when later MOC NA images became available, and compared their presence with two sub-regions of the cryptic terrain: one where the mismatch of dark albedo and very cold temperatures (i.e., "cryptic behavior") occurred between $L_s = 90°$ and the complete sublimation of the seasonal ice cap (the layered deposits and the floor of the Prometheus impact basin), and another "more inclusive" definition which displayed cryptic behavior at any time during the defrosting season (Dorsa Argentia and the southern highlands). All identified spiders fell within the more inclusive version of the cryptic region and the *majority* fell within the more narrowly defined domain. However, spiders were not observed within all parts of the current cryptic terrain; specifically, spiders were found only on the SPLD and not on the southern highlands or residual cap. There appeared to be no special elevation/slope or surface roughness control on the formation of spiders Piqueux et al. (2003). However, these early studies were limited in the spatial resolution and surface coverage available for the survey.

4.2. Spider Morphology in High Resolution: The Development of a Diverse Classification

As discussed above, the very high resolution (50 cm/pixel) imaging by HiRISE provided enhanced spatial resolution, high temporal resolution change detection and through stereo-imaging capability, detailed topographic profiling (McEwen et al., 2007). A focused study of 19 sites containing spiders, including areas within and outside of the cryptic region, confirmed that small-scale topography appeared to be correlated with spider formation (C. J. Hansen et al., 2010). This was particularly relevant for Inca City, which has a wide range of slopes, exceeding 13° in many cases; here, the feedback between morphology and underlying terrain was investigated for the first time. Through a detailed morphological analysis, spiders were categorized based on (a) channel organization, (b) the relationship and scale of channels to their central depression (if any) and (c) tortuosity. Moreover, due to both the growing understanding of different spider "sub-types" and the potential for misinterpretations in the media, a less-colloquial nomenclature was proposed. C. J. Hansen et al. (2010) introduced the term *araneiform*, meaning "spider-like" in Latin, for these features so as to avoid confusion with Earth-based lifeforms and musical works (Bowie, 1972). (As explained above, in this study we apply this term to the diverse range of dendritic morphologies, which includes but is not limited to spiders.)

A key small-scale observation was that channels widened uphill, countering gravity-driven mechanisms and implicating gas as the erosive agent C. J. Hansen et al. (2010). Additionally, in a slight diversion from Kieffer's model, fans and spots were observed to mostly emanate from within channels, as opposed to from within the individual spider centers (C. J. Hansen et al., 2010). Spider channel lengths were measured to be variable, but on the order of tens of meters, and were 1–2 m deep (C. J. Hansen et al., 2010), with channels narrowing away from their centers. In general, many of these features are coincident with polygonal cracks, suggesting that channels may be cracks which became enlarged through the venting process C. J. Hansen et al. (2010); Piqueux and Christensen (2008a, 2008b). Bright drifts of fines were observed to settle within channels—possibly later muting sublimation either due to frost preferentially accumulating on dust acting as condensation nuclei and altering thermal gradient, or by stifling gas flow.

Two main strains of araneiform were identified, based on differences in their morphologies: "Classic spiders" and "Lace Terrain." Lace was identified as dense entanglements of tortuous channels with no observable centers (Figure 1e), while classic spiders are typically isolated entities, and some in the deepest depressions of the Inca City region overlap with their neighbors to the point where separate features are near-indiscernable (C. J. Hansen et al., 2010). By utilizing MOLA topography, lace appeared to occur on gentle slopes, while individual spiders were typically draped upon terrain with slight undulations beneath them. It was suggested that these undulations provided points of weakness which could preferentially be exploited in the ice rupturing process, though this was not explicitly quantified. Temporal analysis revealed that fans and spots corresponding with lace terrain appeared at a much later L_s than those for distinct spiders, suggesting that a more diffuse process may be in operation at the location of lace.

Additionally, there are distinct species within the "classic" strain of spiders. Based on an initial qualitative morphological survey over 19 sites, C. J. Hansen et al. (2010) identified two morphologies: (a) "fat" spiders consist of central depressions with a large diameter relative to the extent of their short, few, wide troughs (Figure 1f), and (b) "thin" spiders have long, thin troughs (Figure 1a). Although no formal, morphometric categorization metrics were applied in the early studies, many observations were noted that may inform their environmental controls. Fat and thin spiders are generally seen in separate areas of differing elevation, often lining up in distinct "chains," although it is unclear if fat spiders can develop into thin spiders through subsequent venting episodes. However, the studied fat spiders had a much higher spatial density (192 km^{-2}) than thin spiders (36 km^{-2}) (C. J. Hansen et al., 2010).

Cementation of substrate was suggested as a potential driver driving the different morphologies (C. J. Hansen et al., 2010). However, despite neutron spectrometer studies identifying near–surface water ice (Mellon & Phillips, 2001; Prettyman et al., 2004) and high latitude patterned ground of putatively periglacial origin (Mangold, 2005; Mellon, 1997) in the south polar regions, the only connection drawn between ice properties and araneiforms thus far has involved identifying araneiform locations (and not specific morphologies) within and outside of the cryptic region (C. J. Hansen et al., 2010; Piqueux et al., 2003; Schwamb et al., 2018). Additionally, owing both to HiRISE's sparse spatial coverage and possibly to the tedious nature of mapping such small-scale features, a comprehensive map showing where these specific sub-categories are located has not yet been made.

Following this work, Hao et al. (2019) added to the inventory of classified spiders by describing two types seen in Inca City: "half" (Figure 1) and "elongated" spiders (Figure 8). They noted that these features were correlated with topography, including ridge boundaries and previously existing linear depressions. Since many spiders of a given morphology appeared relatively evenly spaced within a cluster (C. J. Hansen et al., 2010; Piqueux et al., 2003), the authors suggested that "inhibited zones" exist around spiders, within which another spider is less likely to occur. They then applied a spatial randomness and clustering model (Michael et al., 2012) to evaluate the Mean second Closest Neighbor Distance (M2CND) of seven study regions (Hao et al., 2020) (Figure 9a). The sites were overall found to be ordered and the authors suggested that porosity, permeability and cohesion regulate and modify spatial configuration of a spider population on the regional scale, with pressure release by jetting from one spider diffusing into the substrate over a given distance and inhibiting additional spider formation. However, later work (Attree et al., 2021) showed that most of the gas released in the sub-slab sublimation process runs between the overlying ice and not into the substrate, indicating that the diffusion of gas into the substrate may not be an overarching factor in this specific ordering, at least for larger araneiforms.

L. Mc Keown et al. (2023b) conducted a study over three spider sites containing fat and thin spiders, measuring the diameters of the spiders and their central pits, as well as the number of branches (over 1,000 per spider for starburst spiders) using the Strahler (1952) stream order method for 112 spiders. Informed by their previous experiments of spider development on the small-scale (L. Mc Keown et al., 2021), they suggested that the central pit of spiders corresponded to the size of the original vent responsible for their formation. Because vent velocity scales with X^2, where X is the ratio of vent separation to vent diameter (Kieffer, 2003), they hypothesized that spiders with smaller original vents and distances between operating vents would owe to higher velocities and hence more branched spiders. Their measurements supported this hypothesis, as they found that groups of spiders with smaller distances between them were far less branched than those further apart (normalized to scale). The level of branching of spiders scaled with both the ratio of full extent to central depression diameters and distances between spiders (Figure 9b). This work also identified new spider morphologies (see Figure 8) ranging from "Fan" to "Spiky," "Segmented," "Flowing," and "Sunflower" (Figures 8a–8c, 8e, and 8f).

However, there are other groups of spiders present in these sites, as well as intermixing "species" and interweaving lace terrain. Within these more complex assortments, these morphometrics are not easily collected. Based on the superposition of different "groups" of spiders, it is possible that those with similar morphology and regular spacing may have formed contemporaneously. Areas with less discernible patterns may indicate the formation of spiders over a range of times. Further understanding of the substrate properties as well as insolation receipt and relative ice thickness will elucidate whether specific groups of araneiforms developed at different periods in Mars's recent climatic history.

4.3. Spiders Outside of the SPLD

Seeking to extend the survey of spiders to a wider range of terrains, a study by Schwamb et al. (2018) enlisted the aid of 10,000 citizen science volunteers to inspect 90 CTX images, covering 11% of the south polar regions and

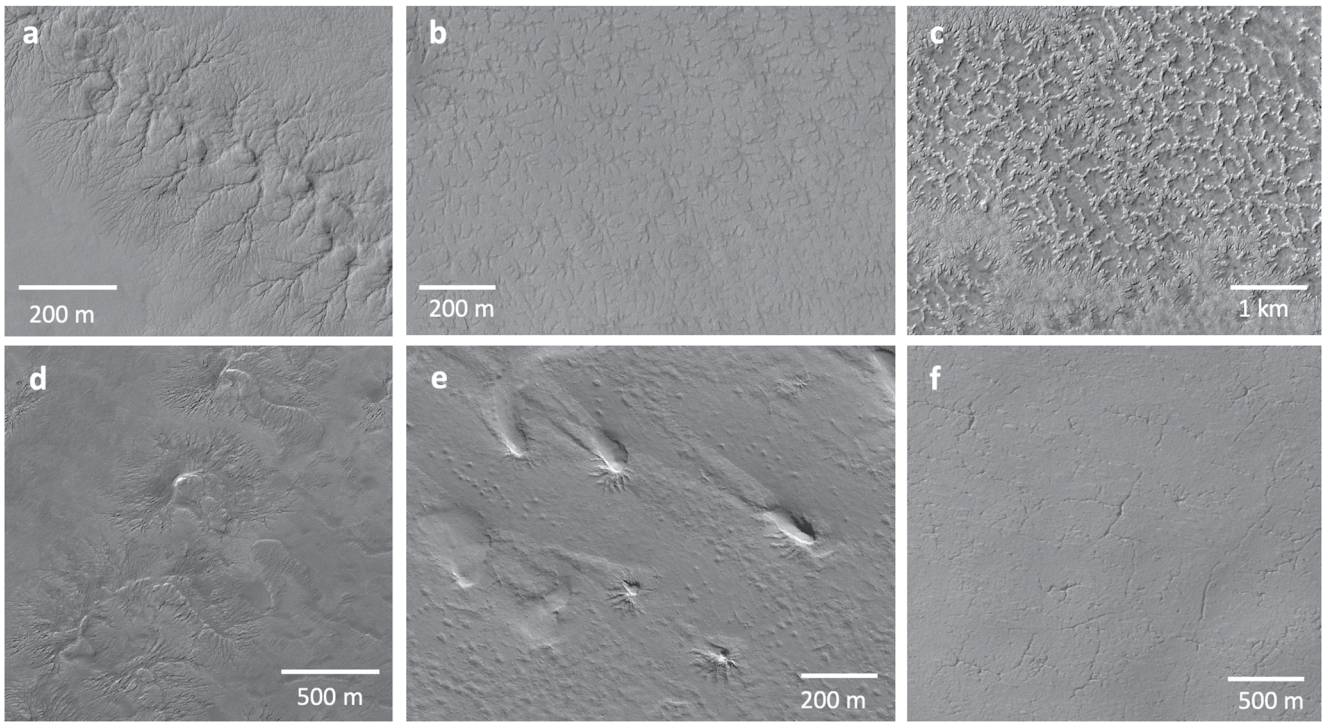

Figure 8. Additional spider morphologies classified in the last 3 years. (a) "Fan spiders" in High Resolution Imaging Science Experiment (HiRISE) image ESP_048777_0990 at lat = −80.67°N and lon = 75.85°E, identified by L. Mc Keown et al. (2023b). (b) "Spiky spiders" in HiRISE image ESP_048777_0990 at lat = −81.8°N and lon = 302.41°E identified by L. Mc Keown et al. (2023b). (c) "Segmented spiders" from the Murray Lab CTX mosaic at lat = −83.378°N, lon = 170.353°E identified by L. Mc Keown et al. (2023b). (d) "Flowing spiders," from HiRISE image ESP_005655_0970 at lat = −83.008°N, lon = 167.586°E identified by L. Mc Keown et al. (2023b). (e) "Sunflower spiders," from HiRISE image ESP_013886_0875, at −87.521°N, 162.39°E, identified by L. Mc Keown et al. (2023b). (f) "Elongated spiders," in HIRISE image PSP_006204_0985, at −81.386°N and 295.052°E identified and described by Hao et al. (2019). North is up in all images and illumination is from the left.

identify spiders and swiss cheese across and outside of the SPLD, spanning Noachian, Hesperian and Amazonian units (Figure 10). Although the full range of spider morphologies was not included, volunteers from the general public were trained to recognize individual "classic" spiders, lace terrain and baby spiders, and validation and statistical analysis was later applied by the Planet Four teams to verify results. 75% of spiders were found on the most recently defined unit of the SPLD (Tanaka et al., 2014), although relative stratigraphy was not explored.

Interestingly, the study revealed 96 spider detections outside the SPLD on terrain including possible ejecta blankets (e.g., the location, Montauk) wherein unconsolidated material may provide an environment conducive to spider development. This work showed a clear separation between swiss cheese and spiders, and also identified terrain with morphology similar to "degraded" swiss cheese.

5. Sand Furrows

Kieffer's model for the formation of spiders was originally applied only to the SPLD. However, HiRISE images of spring activity on the north polar erg surrounding the NPRC show that the model works well to explain northern seasonal activity, specifically the formation of sand furrows (Figures 2 and 11).

The main difference is the surface on which the seasonal ice is deposited, and the way the process plays out on the northern dunes. Pressurized gas underneath impermeable CO_2 ice will seek out and rupture the ice at weak points in a process known as "cryoventing" (M. C. Bourke, 2013). On dunes there are three weak zones:

1. The brink of the dune that sees sunlight first and thus begins sublimating first
2. The flat expanse on the stoss side of the dune, which cracks into polygonal plates, and
3. The interface of the dunes with the substratum (C. J. Hansen et al., 2011, 2013). Figure 11a shows the idealized flow of trapped gas on a dune.

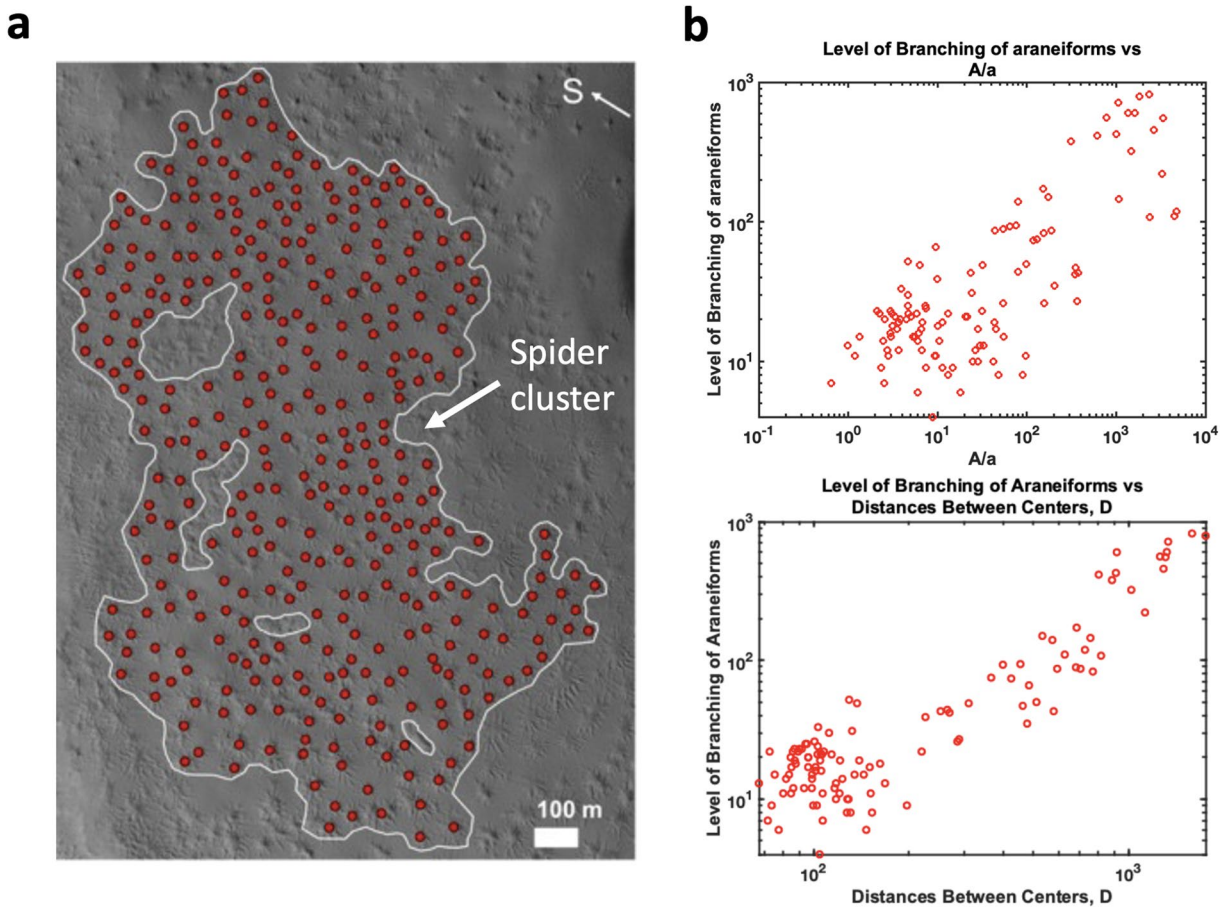

Figure 9. Morphometric studies of spiders which both highlight how certain clusters of spiders exhibit distinct spacing between individual spiders. (a) Image from Hao et al. (2020), who tested spatial randomness for fat spiders in Inca City, noting distinct distances between certain clusters of spiders. (b) Image from L. Mc Keown et al. (2023b), who observed that these distances (*D*) and also the ratio of full extent to the central depression (*A*/*a*) correlated with the level of branching (number of connecting troughs, L. Mc Keown et al., 2023b) of spiders.

Gas is channeled below the seasonal ice layer to the weak rupture points scouring shallow troughs or "furrows" (M. C. Bourke & Cranford, 2011). The furrows were identified within all three types of weak zones, on numerous north polar dunes. The connection of furrows to seasonal outbreaks is documented in C. J. Hansen et al. (2013) and an example is shown in Figure 11c. Boulders represent an additional weak spot—seasonal outbreaks and furrows are also associated with boulders, as shown in Figure 11b.

Although the process of formation is hypothesized to be similar to that of forming a spider, the nature of the substrate is not, which may explain why furrows have some different attributes. Furrows are shallow, branching and networked and they range in planform from sinuous to linear, rectilinear and dendritic (M. C. Bourke & Cranford, 2011). They are typically 1.5 m wide and <0.25 m deep. Length varies considerably depending on dune geometry but may be as long as 300 m; this suggests that sub-ice gas mobilization and transport toward a vent can be sustained over a substantial distance (M. C. Bourke, 2013). Furrows have been detected on 95% of the dunes imaged by HiRISE and are ephemeral. Furrows have been found every year in similar but not identical locations on dune slopes, suggesting erasure by saltation and ripple migration in the summer and fall when the dunes are ice-free and sand is mobile (M. C. Bourke & Cranford, 2011).

Furrows were studied in detail at 10 sites on the north polar erg. This mapping revealed the preference for furrows to form at the base of the slopes, changes in slope, and close to the dune brink–consistent with where the weakest ice was thought to be found. Preliminary results also suggest a latitudinal trend, with a higher density of furrows on more polar dunes, which could indicate a functional dependence on ice layer thickness in vent formation (M. Bourke & McGaley-Towle, 2014).

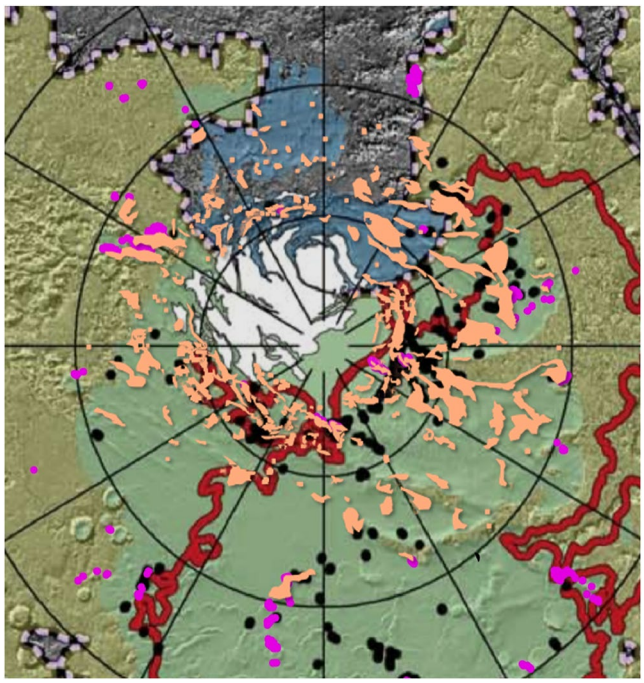

Figure 10. Existing maps of spiders. Black dots show mapping of spider locations with Mars Orbiter Camera by Piqueux et al. (2003). Pink dots show spider locations identified by the Planet Four Citizen Science campaign, where 11% of the south polar region within 75°S was surveyed for spiders with CTX images. Orange polygons denote the most complete coverage of spiders to date. This mapping is ongoing (L. Mc Keown et al., 2022) (at time of writing down to −80°S) and also shows rough spatial coverage of spiders, mapped using the contiguous coverage provided by the CTX Global basemap of Mars (Dickson et al., 2020).

Although first identified in north polar erg images, furrows are also present on dunes in the Southern Hemisphere (SH). Images of dunes in the south polar region from 40°S to 72°S show that furrows are also more numerous on dunes located further poleward (Nash & Bourke, 2015). However, no furrows have been detected poleward of 72°S.

6. Dendritic Troughs

Dendritic troughs were first discovered by G. Portyankina et al. (2017) in overlapping HiRISE images of inter-crater dune fields (see Figure 2 for an example), which are common HiRISE monitoring sites so as to track their extensive seasonal activity (e.g., sublimation spots, fan and blotch deposits, and furrows). Although morphologically similar to furrows and of a similar spatial scale (width of several meters, lengths of tens to hundreds of meters), dendritic troughs remain visible for more than one Mars year and develop over time into more complex dendritic patterns. This evolution in their form indicates that dendritic troughs are being actively carved into the permanent substrate, which also differentiates them from large spiders that, so far, have not been observed to expand or otherwise change. Dendritic troughs have been observed to be actively modified under the current climate conditions, and have regular seasonal fans and blotches associated with them. These correlated activities provide additional general confirmation to the Kieffer model (Section 2).

Although dendritic troughs have been hypothesized to be related to spiders, it remains unknown if the dendritic troughs observed today will eventually evolve into large spiders, and hence whether we can apply rates of dendritic trough erosion to large spiders. Additionally, why is activity observable in the dendritic troughs but not in spiders? One explanation for the fast pace of dendritic trough development is that they are near dunes that can serve as a source of loose sand, which is an excellent erosion agent and thus can efficiently and signficantly accelerate substrate erosion.

7. Numerical Models of Araneiform Formation

Kieffer's model described the formation of araneiforms in several distinct steps or sub-models (as discussed in Section 2) that readily lend themselves to numerical modeling. Naturally, the first numerical models associated with araneiform formation were calculations of the plausibility of the whole Kieffer model and appeared virtually

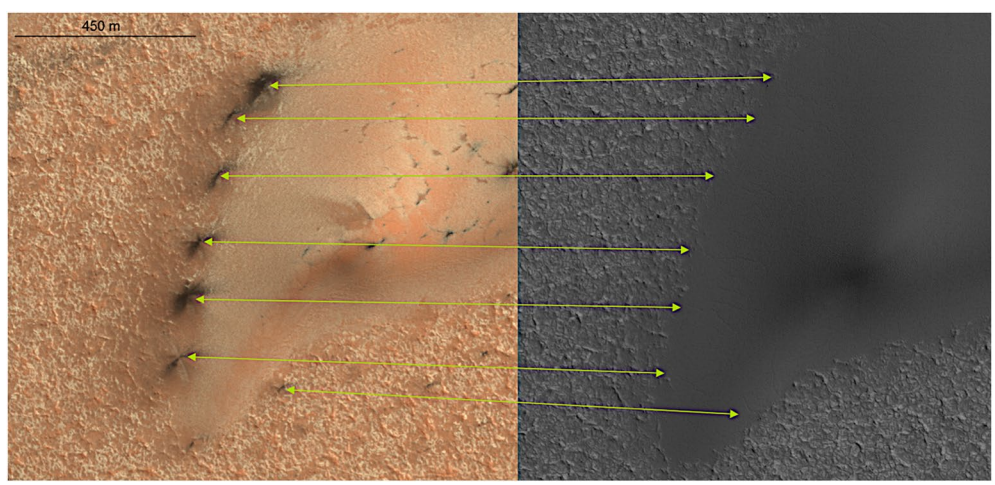

Figure 11. Seasonal outbursts can be mapped to furrows reaching the edge of the dune and erupting at weak spots at the interface of the dune with the surface. (Left) ESP_016111_2600 taken at L_s 32.5; (Right) Furrows are visible in ice-free image ESP_018445_2600 taken at L_s 113.2.

simultaneously with its first publication. Since then (i.e., since the early 2000s), there have been multiple models to describe araneiform formation via gas jetting and the conditions under which it is possible. Below is a simple classification of the involved processes that have been modeled:

7.1. Models of the Eruption Conditions

- Modeling of the energy budget on top of the seasonal CO_2 ice

  Depending on the desired spatial scale and level of details, numerical calculation of the energy budget at high latitudes get tricky and counter-intuitive, especially during seasons with fast changes in daily solar angles. The transition from polar night in early spring is characterized by spikes of daily solar energy input on equator-facing slopes, potentially leading to preferential jet eruptions on those illuminated slopes. This does not necessarily lead to araneiform creation on those slopes because surface properties, in particular surface stability when considering sloped terrains, are as important to erosion efficiency as strength and amount of jetting activity. Later in the season, the energy becomes more evenly distributed between slopes of different orientations, with polar-facing slopes getting the lowest partition of the incoming daily sunlight. During polar day, all slopes get illuminated during some part of the day. The calculations of energy input were done for idealized slopes (Byrne, 2009) and for specific locations with Digital Elevation Models (DEMs) (G. Portyankina et al., 2010). These models can take into account atmospheric absorption and scattering; however, up to now only idealized atmosphere conditions were used. Using OMEGA near infrared observations, Schmidt et al. (2009, 2010) modeled CO_2 mass balance for the cryptic and anti-cryptic region, noting that the seasonal cap recession is not symmetric around the south pole. They found that mass balance was related to albedo and that after $L_s = 220°$, the sublimation of the anti-cryptic region was stronger than that in the cryptic region. However, the lack of localized data on cloud and fogs, as well as dust content in early spring, prevents more detailed atmospheric correction models from being used.

- Modeling of heat transfer inside the top of the substrate

  Aharonson (2004) modeled the propagation of seasonal heat waves inside the top layer of a polar substrate. A simple 1-dimensional thermal diffusion model showed that the heat deposited in the exposed ground during the summer could support very early basal CO_2 sublimation. Thus, the formation of spots and fans was considered to be possible during the earliest parts of spring, before the sun has risen sufficiently high above the horizon to supply significant heat and clean the slab of impurities.

- Modeling of light and heat transfer inside the seasonal ice

  After the sunlight hits the top of the seasonal ice layer, it gets partially reflected back into the atmosphere and partially scattered toward the bottom ice boundary where it meets the substrate and gets absorbed. This process was modeled by Pilorget et al. (2011). A regolith-CO_2-atmosphere column was simulated and a coupled light and heat transfer model was used to determine when and where basal sublimation of CO_2 would occur on Mars. Simulation results show that the occurrence of basal sublimation mainly depends on the CO_2 ice properties, namely how clean and transparent the ice is, and not on the properties of the substrate such as thermal inertia or surface slope toward/away from the sun. The timing of jetting activity, however, is sensitive to all the above mentioned parameters.

- Modeling sublimation beneath the ice sheet and the stresses it induces in the ice.

  G. Portyankina et al. (2010) calculated the amount of CO_2 ice that sublimes underneath the seasonal ice layer when the first rays of sunlight reach it after the polar night. The sublimation happens quickly and the gas pressure created by the sublimation rises exponentially in minutes and in some cases—for example, on equator-facing slopes—even seconds. The pressure creates strain in the ice shield. The point of mechanical failure for the ice sheet was calculated by G. Portyankina et al. (2010) as a proxy for the timing of the first jet eruption. According to the model, at latitudes between 75° and 85° they are expected to occur within minutes to seconds after the local sunrise. These simulations used mechanical properties for water ice to describe CO_2 ice for the simple reason that neither Young's modulus nor yield strength are known for CO_2 ice (see Section 14 for discussion about CO_2 properties). Our current understanding is that the CO_2 ice properties vary depending on the form of ice, that is, crystalline or amorphous, as well as the type of crystalline structures. In addition, in every laboratory experiment so far, CO_2 ice was observed to extensively crack. Early spring cracks in the seasonal layer were also observed on Mars (G. Portyankina et al., 2012). For the mechanical stability calculations, the presence of cracks has dual influ-

ence: cracks make the ice sheet much weaker, and also provide escape paths for growing pressure. Thus, the exact eruption timing has a very large uncertainty due to the lack of knowledge on CO_2 sheet properties and quality.

Attree et al. (2021) extended the model for the mechanical stress and resulting failure of the seasonal ice sheet by including the flow of CO_2 underneath the ice either through a cavity or a permeable regolith layer. The model estimates show that a centimeter-sized cavity is sufficient to supply a free gas flow for the previously estimated flow rates expected under polar spring sublimation conditions. Such a cavity can be easily produced by either levitating an ice layer or bending it by the growing gas pressure.

7.2. Models of Jet Eruption From a Pressurized Reservoir Into Low Martian Atmosphere

A distinctive (and probably the most organic) type of model for araneiform formation deals with active eruptions of the jets. These are typically fluid dynamics models of pressurized gas erupting into the Martian atmosphere. The model has to account for the correct Martian conditions of low gravity and low atmospheric pressure as well as temperature regime typical for local early spring. It may or may not include dust particle transport by the jet and consequent formation of the fan (or blotch) deposits.

- Ballistic approach for deposition patterns

  First, to understand the formation of seasonal dark deposits, N. Thomas et al. (2010) calculated the distribution of dust and regolith particles expelled upwards by a jet and then deposited onto the bright seasonal cap using a simple ballistic approach and an estimate of atmospheric drag. The resulting fan deposits are a reasonable approximation of the observed fans. The ejection velocities that fit the observation were in the range 10–20 m/s with an angular ejection profile of <6°. This model also tackled estimates of the mass of particulate material deposited by the jet and jet eruption duration. Unfortunately, both of these appeared to strongly depend on the model parameters, which can only be weakly constrained.

- Fluid dynamics models

  The deposition pattern of a fan or a blotch depends on the structure of the jet that createdit, which in turn is determined by the state of the atmosphere it erupts into and the eruption parameters such as gas flux, particulates loading, duration of the eruption, etc. N. Thomas et al. (2011b) used existing computational fluid dynamics code to study a steady-state jet eruption under martian atmospheric conditions to evaluate the structure and distribution of dust and sand particles within the jets for a range of input parameters. Steady-state in this case means that the system balances pressure in the cavity underneath the ice sheet and sublimation rates from the lower ice boundary. The model calculations have confirmed that small (5–25 m in length) fan deposits can be produced by a steady-state outgassing, but larger fans (also observed in several locations within SPLD) will require a transient eruption. Transient in this context describes an explosive process that releases the over-pressurized gas from the under-ice reservoir.

Another step up in the complexity of the same model was published by N. Thomas et al. (2011a). The model was run for a larger and more inclusive range of parameters. One of the many interesting results of this modeling work is that a jet erupting on a slope and a jet erupting under windy conditions create morphologically distinct fan deposits if the rest of the jet parameters are set the same (vent geometry, ice over-burden pressure, dust load inside the jet etc.). However, given the wide and mostly unknown span of these parameters, it is possible to recreate similar patterns with different sets of parameter. It is unlikely that the currently available imagery provides adequate constraints to allow unique solutions for jet properties.

7.3. Models of Fractal Pattern Formation of Araneiforms

The dendritic quality of many araneiforms, especially large and well-developed ones, suggests that their formation is governed by stochastic/probabilistic phenomena. Thus, the creation of araneiform patterns can be modeled with a two-dimensional Diffusion-Limited Aggregation (DLA) model that describes the formation of dendrite shapes by mathematical probabilistic means (G. Portyankina et al., 2020). This type of probabilistic model can never recreate the exact shape of an existing araneiform, but it can produce shapes in the mathematically similar parameter space, that is, with the same order of tributaries, tributary densities, and bifurcation ratios (terms commonly applied to other dendritic structures such as terrestrial rivers and—by extension—to araneiforms). The DLA model, with a changeable governing probability field, was able to reproduce the variety of araneiform shapes observed on Mars.

Additionally, the DLA modeling showed that the preexisting small-scale topography and nearby large-scale topography determines— or at the minimum greatly influences—the shapes of the resulting araneiforms.

7.4. Limitations and Missing Models

Models of active jet modeling currently only consider steady-state eruptions; models of transient dynamics, such as when the jet breaks through ice, have not yet been attempted. In addition, no modeling of surface erosion underneath the ice layer has yet been attempted. A direct link should be describable between the fluid dynamic modeling of jet eruptions and the erosion and resultant morphometrics of araneiforms, but this link is still not well-understood.

Some modeling of the simultaneous creation of multiple araneiforms and araneiform fields was discussed in G. Portyankina et al. (2020). However, the physical model approach of this task was not yet addressed. The distribution and release of gas over-pressure below the seasonal ice sheet is an important factor in creating the spacing between spiders, and probably in shaping spiders themselves, particularly for those formed contemporaneously, as discussed in Section 4.

Finally, we need to note the limitations all models naturally possess because a model is only as good as its assumptions coupled with precision in the current knowledge of its input parameters. Many models rely on lab-derived empirical properties of materials. As these properties are constrained from empirical data acquired from laboratory experiments, and as spacecraft observations advance, so too should the relevant models (Figure 12).

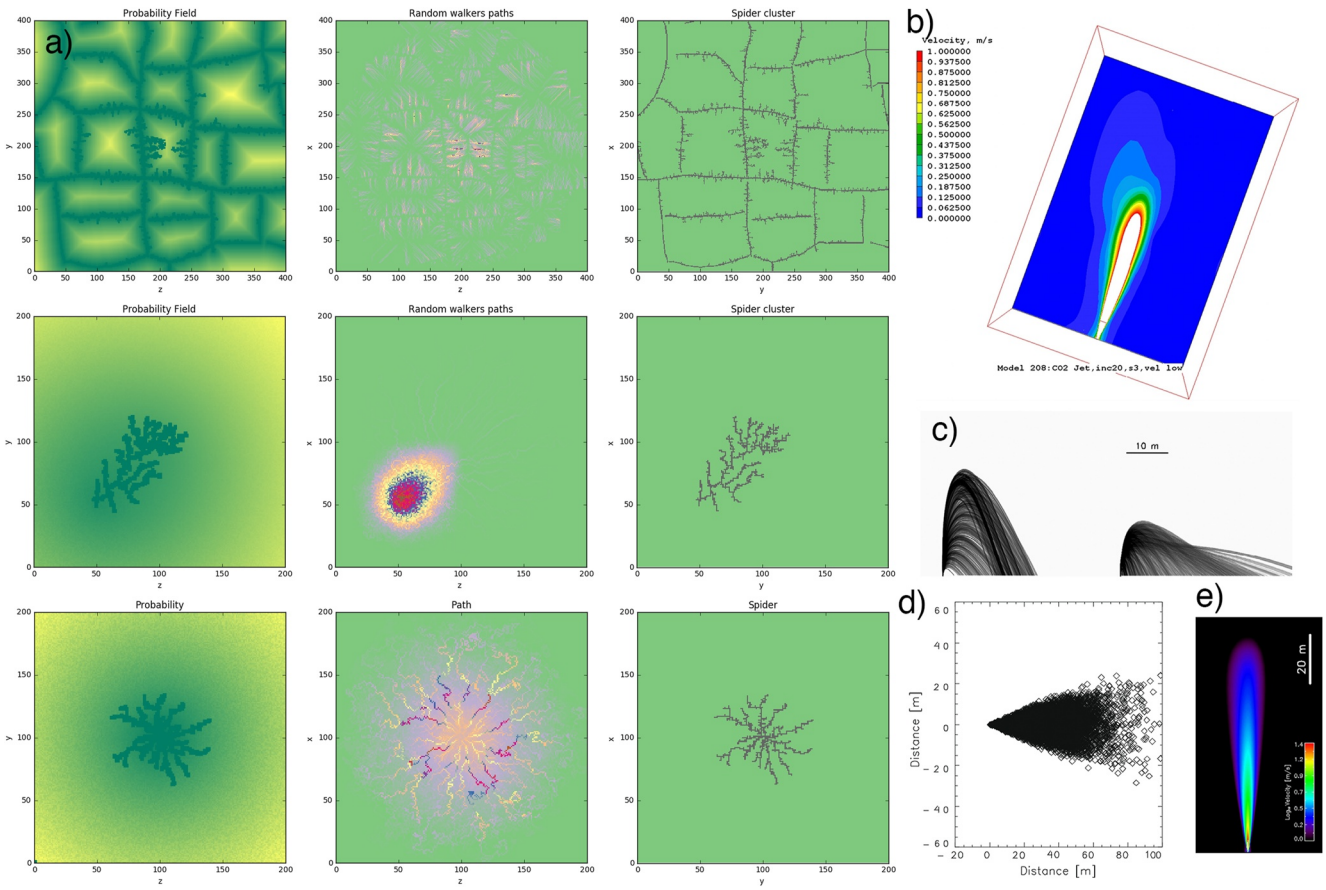

Figure 12. Examples of computer models related to araneiform formation: (a) runs of the Diffusion-Limited Aggregation model for three different governing probability fields. Image from G. Portyankina et al. (2019). Top to bottom: pre-existing topography from polygonal terrain, asymmetric probability field, and a centrally symmetric one vent araneiform. (b) Magnitude of the gas velocity in a model of the dusty CO_2 gas jets using a computational fluid dynamics code from N. Thomas et al. (2011a). (c) Dust particle trajectories in the jets. Left and right panels show identical entry conditions. The left has no wind but has a 20° slope. The right one has no slope but a 6 m/s wind from the left. Particle height is affected by the wind. Note also how the trajectories are modified by the wind, thereby influencing where particles of different sizes are deposited. (d) Result of a ballistic calculation for a jet-like plume of large particles on a slope: the surface tilt used was 20°, emission velocity was 15 m/s, and the spread at the vent was set at ±3°. Emission was normal to the surface. (e) The velocity field generated by a 170 g/s outflow almost reaches the top of the domain (150 m from the surface). Images (b–e) are from N. Thomas et al. (2011a).

8. Lab Experiments of Araneiform Formation

As has been described, the CO_2 condensation/sublimation cycle responsible for Martian araneiforms has no terrestrial likeness and this limits our intuition regarding the processes forming these features. To address this, analysis of remote-sensing observations of planetary geomorphology and numerical modeling extrapolations are used to guide small-scale empirical observations of physical dynamics under simulated planetary conditions. This approach enables direct observation of analogous new physical processes involving phase transitions and their interaction with materials under extreme regimes not naturally available on Earth, with careful tests and calibrations as experimental results are applied to the broader picture. Experimental studies designed to acquire measurements of material properties and physical parameters are also being utilized to tune models to Mars conditions, as mentioned in Section 7. Such work has motivated a paradigm shift in our understanding of processes that have no Earth analog, revealing many processes that may not have been imagined before such as "levitating water pellets" (Raack et al., 2017), vigorous CO_2 sublimation dynamics (L. Mc Keown et al., 2021) and metastable boiling water (Massé et al., 2016), all prompted by efforts to understand mass-wasting processes on present-day Mars. As this paper reviews the study of araneiforms, we focus mainly on those that have advanced our understanding of dendritic feature formation, as well as related CO_2 ice dynamics and properties.

8.1. Experiments Outside of Planetary Simulation Chambers

Some groups have been able to investigate certain elements of CO_2 dynamics and araneiform formation on Mars without the use of planetary simulation chambers, which can be costly to run and hard to access. Laboratory experiments by de Villiers et al. (2012) showed that the characteristic radial dendritic patterns of araneiforms could be developed by the erosive venting of gas through a hole in the upper plate of a Hele-Shaw cell filled with unconsolidated granular material (Figure 13a). Although the experiments did not simulate patterns formed by sublimating CO_2 ice, as is hypothesized for Mars, they indicated that branched channels could form in a granular bed by convergent flow driven by an evenly distributed over pressure, toward a "vent" in an overlying impermeable sheet, as proposed in the Kieffer model.

Following this work, Diniega et al. (2013) observed that channels formed beneath a CO_2 ice block when placed on sandy substrate during field tests for linear dune gully formation at Coral Pink Sand Dunes in Utah. Although not formed in the low humidity, pressure, temperature and gravity conditions experienced in the polar and midlatitude regions on Mars, these patterns were observed to be similar to sand furrows. These field experiments, designed to investigate linear dune gully formation by sliding CO_2 blocks, also showed that sublimating CO_2 in contact with a sandy surface was capable of transporting sediment, though this mobilization was also aided by block movement (Figure 16d). Later, work by L. E. Mc Keown et al. (2017) utilized a custom-made low humidity chamber to show that the interaction between sublimating CO_2 ice blocks and granular substrate can generate features similar in morphology to sand furrows, as vents operated at the sides of the ice blocks (Figures 13b and 16c). The disparity in gravity was accommodated by applying a mathematical scaling relationship for grain size. A variety of patterns were observed, as is common for sand furrows on Mars, ranging from linear to sinuous to dendritic. Patterns were most dendritic when fewer vents were operating at once and more area of the surface was covered by furrows when finer grain sizes were used. These experiments also explored the volumes of sediment that could be excavated by burrowing in situ CO_2 ice blocks and resulting morphologies related to linear gully pits (Figure 13b), and calculations of these volumes were used to show that volumes excavated in linear gully pits on Mars were linked to CO_2 sublimation. However, laboratory observations alone are limited in scale and robust numerical modeling is required to extrapolate measurements to Martian scales.

8.2. Experiments Within Planetary Simulation Chambers

A variety of experimental chambers are available (Figure 14) (e.g., Green, 2001; Holstein-Rathlou et al., 2014), which generally have capabilities designed to simulate the low pressure, low temperature regimes typical of planetary bodies which have tenuous atmospheres. These vary in scale, including the 8 m long and 2.5 m wide Aarhus wind tunnel and the 0.6 m long and 0.45 m wide the JPL Extraterrestrial Materials Simulations Laboratory (EMSiL) chamber. Many of these facilities are equipped with a liquid nitrogen solenoid-controlled cooling plate, capable of operating at CO_2 condensation temperatures for direct deposition of CO_2 ice. Those having a cylindrical and back liquid nitrogen shroud provide the advantage of creating a "cold sky" for a minimal temperature

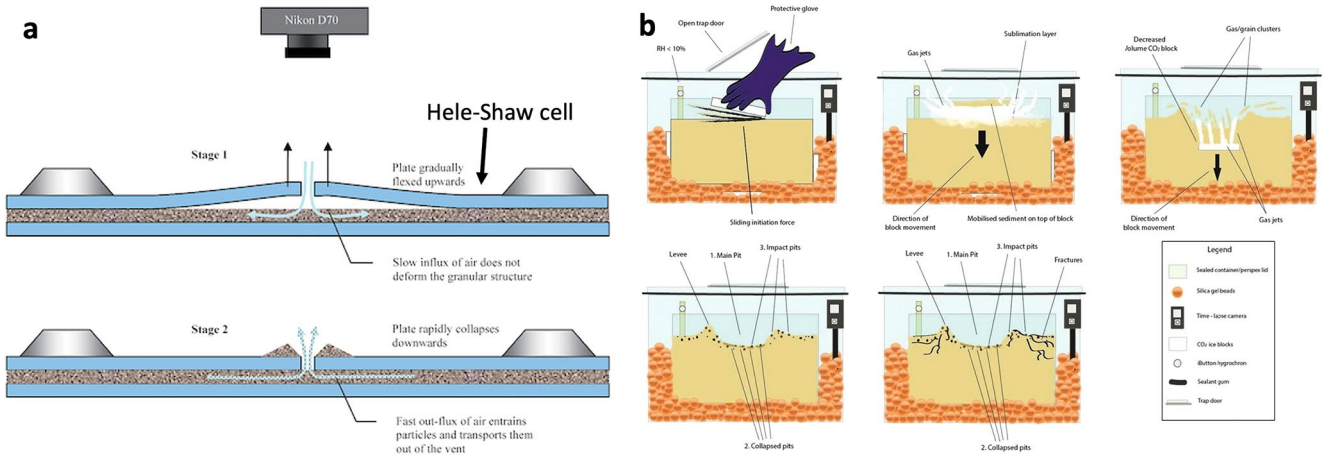

Figure 13. Examples of custom laboratory setups that have not used planetary simulation chambers and demonstrated patterns formed by the interaction between gas mobilization and granular substrate on Mars, on a small-scale. (a) Image from de Villiers et al. (2012), who cycled a glass plate overlying granular material in a Hele-Shaw cell to generate dendritic patterns. (b) Image from L. E. Mc Keown et al. (2017), who flushed atmospheric water vapor from a glass container containing a trap door and used finer grain sizes than those expected on Martian sand dunes, in order to investigate the morphologies produced by sublimating CO_2 ice blocks in situ on granular substrate.

gradient between an icy surface and a simulated "atmosphere." Various types of vacuum pumps can be used to evacuate the chamber of air, reducing pressures to the sub-10 mbar ranges that approximate Mars polar winter and spring atmospheric pressure.

All of these chambers are equipped with feed-throughs, via which data acquisition, image capturing or lighting instrumentation can be attached. Typical methodologies that can be exploited to study CO_2-regolith sublimation processes under Martian environmental regimes include exploring surface volume change through building three-dimensional DEMs with Structure from Motion (Westoby et al., 2012) and investigating ice crystal structure with microscopes (e.g., G. Portyankina et al., 2019). To mimic the Solid State Greenhouse Effect, icy materials can be insolated with solar simulators, which are capable of providing varying radiation intensities and closely matching the spectral distribution of sunlight outside the Earth's atmosphere (e.g., Kaufmann and Hagermann, 2017; Kaufmann et al., 2006). To investigate the interaction between sublimating CO_2 ice and granular substrates, Mars regolith simulants, such as JSC-1A and MGS-1, are generally utilized. When experimental data are used to refine models, glass spheres are preferred for their unimodality.

Many experimentalists have formed CO_2 ice in the laboratory for the purposes of (a) acquiring physical input parameters for numerical models of seasonal processes, including araneiform formation on Mars; (b) supplementing remote-sensing multi-wavelength observations of CO_2 ice on Mars; and (c) observing the interplay between sublimating CO_2 ice and mobile substrate, for comparison with change-detection imaging.

8.2.1. Ice Properties

Studies to obtain optical and mechanical constants and observe CO_2 reflectance and transmission spectra were initiated in the 1960s and continued throughout the 1980s. These are reviewed in Warren (1986). Many of these campaigns were in an attempt to explain satellite measurements of radiation emitted and reflected by observations of the Martian surface. For example, following thermal modeling by Leighton and Murray (1966), which indicated that the Martian atmosphere is composed predominantly of CO_2 and that the Martian polar ice caps must consist at least partly of CO_2 (which had not yet been positively identified in astronomical spectra), experiments by Kieffer (1968, 1970) measured the first comparison spectra encompassing likely frost types on Mars. Kieffer (1968, 1970) cooled a chamber by immersion in liquid nitrogen, trichlorofluoromethane or n-propyl alcohol to measure both gaseous CO_2 and H_2O transmission spectra and solid CO_2 and H_2O infrared reflectance spectra of different compositions and physical characteristics that may have existed on Mars. They found that the addition of small concentrations of water within CO_2 frosts made significant changes in CO_2 spectra and that this effect increases with grain size, making identification of CO_2 difficult with even 10% concentration of H_2O.

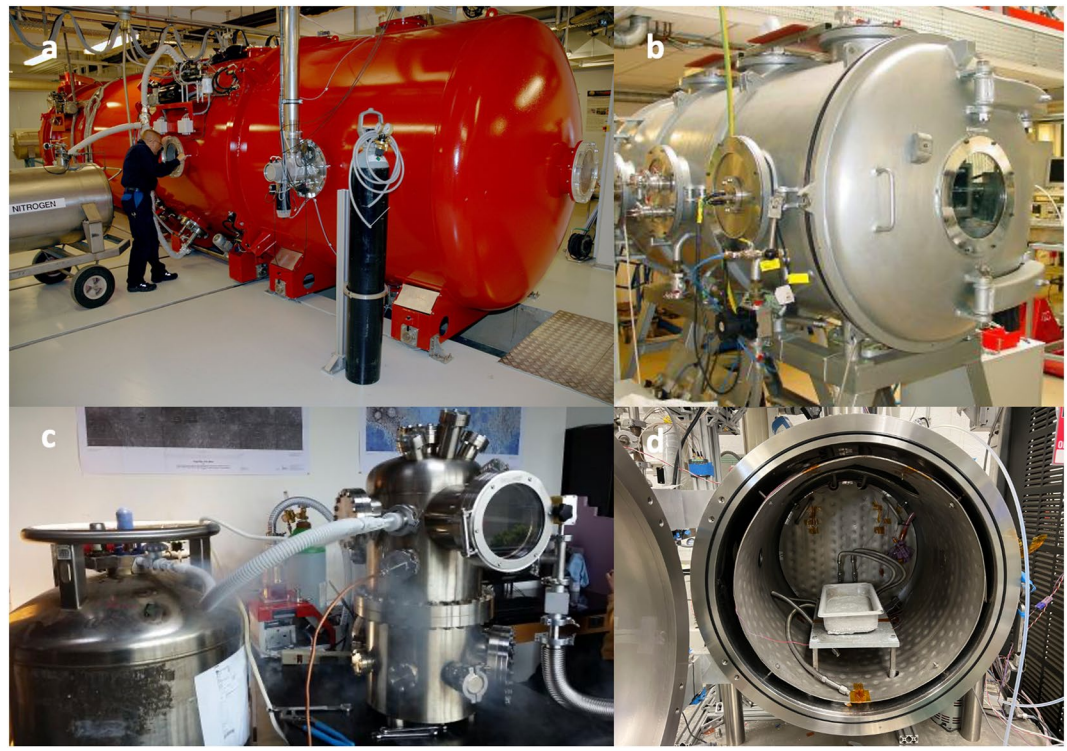

Figure 14. Planetary Simulation Chambers within which analog lab experiments relating to araneiform formation have been performed. (a) Shows the Aarhus Mars Simulation Wind Tunnel located at Aarhus University in Denmark. Source: Aarhus University (https://projects.au.dk/marslab/). (b) Shows the Mars Simulation Chamber at The Open University in the UK. (c) Shows the MARVIN chamber developed by the Smith group at York University and (d) shows the Extraterrestial Materials Simulations Laboratory chamber at the Jet Propulsion Laboratory.

A common complication of optical tests of CO_2 (as well as some other low-temperature compounds) is the size and optical quality of the samples. The procedures for growing high quality, homogeneous samples are well established for up to mm-sized samples. However, CO_2 happens to be highly transparent and thus a mm-sized optical path would not create efficient absorption to accurately measure transmission spectra. Additionally, a second common complication is that, after a sample is created, it is difficult to assess the quality of the sample since it can not be easily removed from the environmental chamber and handled without it starting to sublime.

Thicker slabs of translucent CO_2 ice were later condensed by Ditteon and Kieffer (1979) and G. B. Hansen (1997, 2005) (1.6 and 107.5 mm) to improve upon existing infrared transmission spectra within the infrared and ultraviolet. Using optical constants derived from G. B. Hansen (1997, 2005), in developing the model for cold jetting in araneiform formation, Kieffer (2007) could estimate penetration depths of solar energy into CO_2 slabs. These calculations estimated, for example, that under typical polar summer conditions, 75% of solar energy will penetrate the 0.6 m base of a 940 kg m^{-2} pure solid CO_2 slab, whereas thermal flux is reduced to 50% in 3.7 mm. Blackburn et al. (2010) later experimentally measured the sublimation rate of CO_2 ice of various grain sizes under Martian conditions and concluded that sublimation rate is dominated by heat transfer, and thus is solar-irradiance and optical-depth limited, consistent with dynamic models of CO_2 sublimation. Chinnery et al. (2020) later empirically measured the penetration of broad spectrum solar radiation for the wavelengths 300–1,100 nm into granular CO_2 of different grain sizes and built an empirical model to show that penetration depth increases in a predictable way with grain size and ice composition. This work found that the penetration depth is greater for CO_2 ice than for water ice. The authors also measured this depth for snow and sintered snow, showing that light propagates by scattering at grain surfaces as opposed to direct transmission, regardless of whether the ice is composed of H_2O or CO_2 (Chinnery et al., 2019).

Rheological experiments on CO_2 ice, such as those by Durham et al. (1998) and I. B. Smith et al. (2022), have generally focused on understanding CO_2 glacial flow rates. In these studies, physical parameters of the strength of

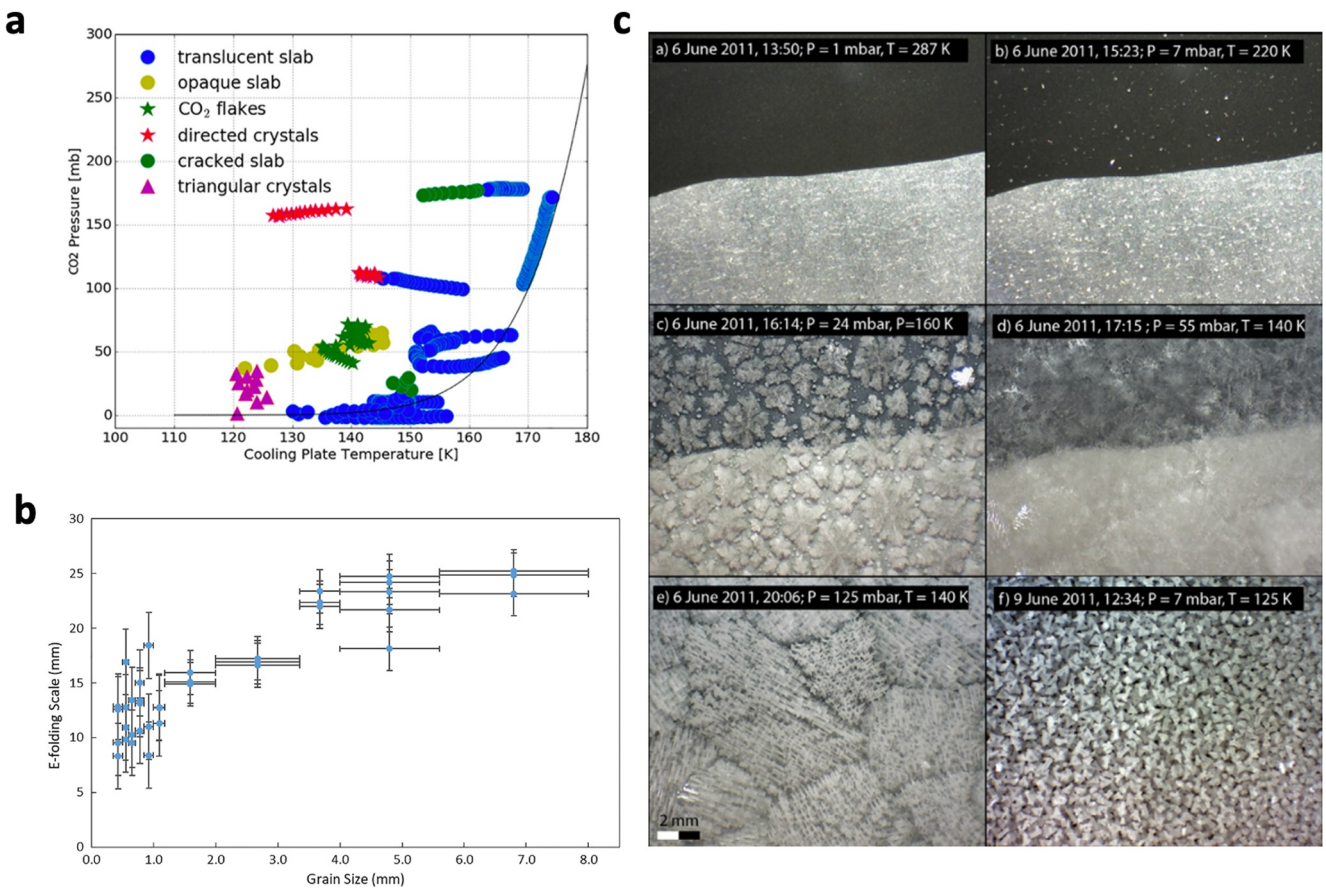

Figure 15. (a) Quantitative measurements of the physical state of CO_2 ice under Martian conditions. Plot of different CO_2 textures (depicted visually in (c)), and the corresponding temperature and pressure ranges under which they condense. Images from G. Portyankina et al. (2019). (b) Shows e-folding scale increasing with increasing CO_2 ice grain size, as observed in experiments performed by Chinnery et al. (2020). Plot from Chinnery et al. (2020).

CO_2 ice slabs, such as the hardness, Young's modulus, and yield strength, are difficult to measure, again, because the ice sample can not be easily handled inside the chamber. One measurement of CO_2 yield strength (desperately lacking in the literature and wanted in models) was done by Kaufmann et al. (2020) under Martian temperatures, using a Leeb hardness tester and calculating the corresponding yield strength. CO_2 appeared to be weaker in these tests than water ice; however, the characterization of sample quality remains an open question. Further, G. Portyankina et al. (2019) conducted experiments that characterized textures of condensed CO_2 within discrete temperature and pressure ranges including relevant to Martian polar regions (Figure 15). Under these conditions, CO_2 ice can be deposited in different crystal forms that, inevitably will have different physical properties and these different properties may be linked to different types of araneiform morphology and activity levels.

8.2.2. CO_2 Ice Processes

While the aforementioned studies contributed vital physical parameters needed to tune models for CO_2 dynamics on Mars, other work has made advancements in validating the Kieffer model on the laboratory scale. Kaufmann et al. (2006) investigated the Solid State Greenhouse Effect, a vital component of the Kieffer model, by shining a solar simulator on transparent media (glass spheres and water ice) under cryo-vacuum and atmospheric pressure conditions, and measuring temperature distributions inside the samples. This work showed empirically that a maximum temperature was possible below the surface of an optically transparent medium when the radiation source is similar to the Sun and with constant temperature gradient. The study also showed that a maximum temperature can be identified below the surface of ices with "moderate" optical transparency, such as ice which is cracked. These authors later used self-produced CO_2 slabs to investigate the solar influence on CO_2 ice layers sandwiching JSC-1A Mars simulant of grain sizes similar to those expected within the SPLD (Paige & Keegan, 1994). When coarse dust grains of <1 mm were used, dust sank via localized sublimation and

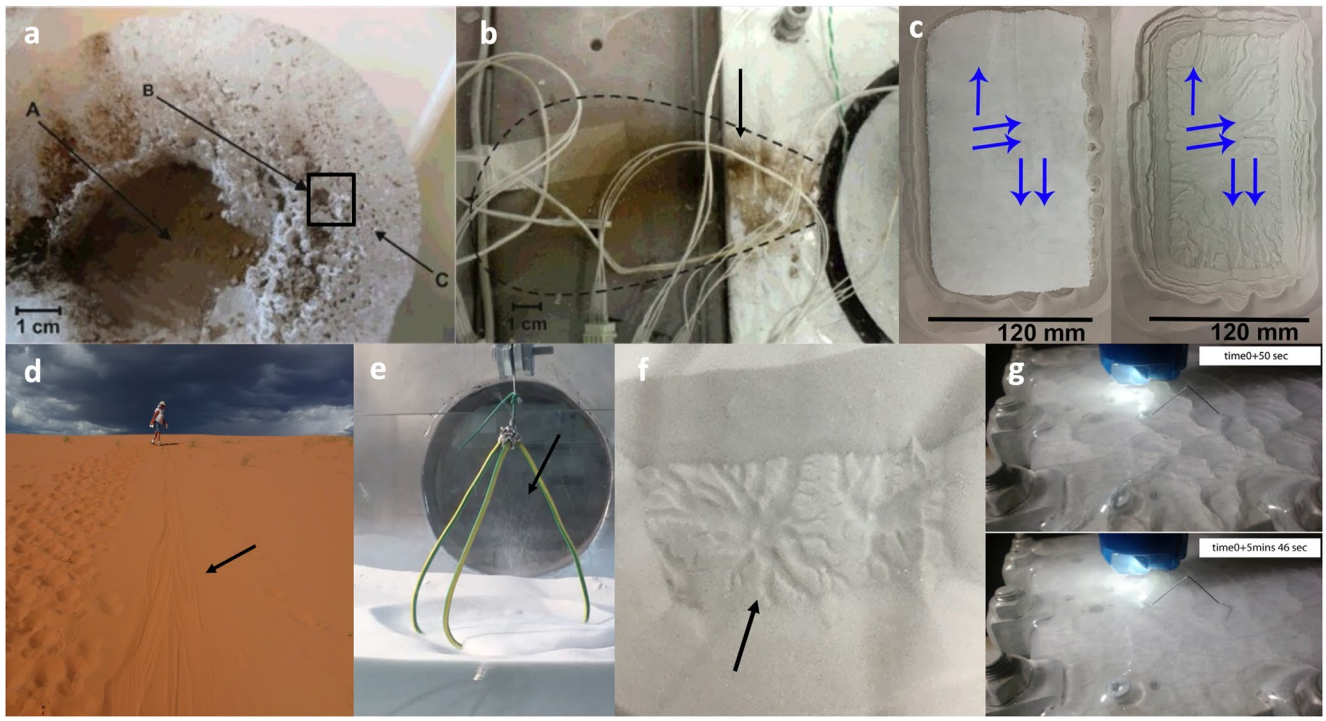

Figure 16. Examples of experimental work performed within experimental chambers and in the field that has advanced our understanding of araneiforms, the Kieffer model and CO_2 properties. (a) Image from Kaufmann and Hagermann (2017), who observed "columns" formed by grains <1 mm sinking via localized sublimation in water ice insolated with a solar simulator under Martian pressure conditions. (b) Image from Kaufmann and Hagermann (2017), who also observed dust of grain size <53 μm lifting from an interface between two CO_2 ice blocks, to outside the system when insolated with a solar simulator under Martian pressure conditions. (c) Image from L. E. Mc Keown et al. (2017), who observed furrow patterns formed via gas venting from the sides in the blocks when a CO_2 ice block was placed in direct contact with a granular substrate under low–humidity conditions. (d) Image from field work performed by Diniega et al. (2013) involving sliding CO_2 blocks down dune lee slopes at Coral Pink sand dunes in Utah. The authors observed that a combination of sublimation and bulldozing effect of the block motion was capable of eroding channels. (e) Image from L. Mc Keown et al. (2021), who placed CO_2 blocks with central vents in contact with granular substrate under Mars pressure conditions and observed that plumes formed and araneiform patterns developed as in (f). (g) Image from G. Portyankina et al. (2019), who investigated the temperature and pressure ranges over which translucent slab CO_2 ice condensed under typical Mars polar conditions. Due to the thermal gradient between the "atmosphere" and surface of translucent ice, the ice cracked and healed over short timescales.

caused "channels" to form through their downward motion within the ice, as was predicted in the Kieffer model (Figure 16a). For grains <53 μm, lifting occurred, in some cases ejecting the encased dust outside of the ice system (Figure 16b) and this showed that dust grains within CO_2 ice could be mobilized simply by localized sublimation induced by the penetration of simulated sunlight, which is a central tenet of the Kieffer model. However, while ice grain size was explored, depth to larger scales was limited by the small experimental setup. Additionally, the degree to which porosity and translucency of ice affects penetration depth and hence dust mobilization has not been explored, which could help to inform why araneiforms have a wide range of morphologies.

The Kieffer model was later investigated and "jets" and small-scale araneiforms were produced for the first time by L. Mc Keown et al. (2021) (Figures 16e and 16f). This work observed the Leidenfrost Effect (Leidenfrost, 1966), wherein a substance that comes in contact with a surface hotter than its sublimation point will sublimate and levitate on a gaseous layer, when placing CO_2 ice blocks in contact with granular material under Mars pressure ranges. By generating DEMs via Structure from Motion (Westoby et al., 2012) of the features produced, this work found that araneiforms were more dendritic with (a) finer grain sizes, (b) smaller vent diameters and concluded that araneiform morphology is governed by gas velocity at the vent and the Shield's Parameter. Furthermore, this work showed unexpectedly vigorous fluidized sediment sublimation dynamics when a block was allowed to burrow and sublimate within the bed under Mars pressure, indicating that CO_2 sublimation is a highly efficient agent of sediment transport. However, the authors used blocks of maximum diameter 20 cm to perform their experiments and this incurred edge effects during sublimation, which would not be relevant on Mars where meters-wide ice blocks have been observed (Dundas et al., 2012). Furthermore, gradual warming of the substrate and diffuse sublimation as on Mars was not explored as room temperature substrate was used to engender the Leidenfrost effect at the base of each block. Future

repeat experiments with a condensed conformal layer of CO_2 and Mars polar temperature ranges will fully explore the range of araneiform morphologies and the environmental parameters which can affect sublimation dynamics.

As well as experiments designed to directly probe the Kieffer model, tangential seasonal analog experiments under Martian atmospheric conditions have elucidated a range of unusual phase-change dynamics on present-day Mars, which may be relevant for araneiform formation. Such experiments are often essential in order to observe fluid dynamic behavior in an unfamiliar environment, with models unable to fill in the gaps of our knowledge without direct empirical observation. Sylvest et al. (2016, 2018) conducted the first experiments to demonstrate mass-wasting triggered by CO_2 sublimation under Mars conditions. Though this movement was also driven by gravity, being aided by varied slope angles in the context of gully and slope streak formation, the experiments showed that slab ice is not necessarily needed to instigate sediment mobilization. Furthermore, through measuring the amount of material transported by photogrammetry, the experiments indicated that grain size distributions imposed a control on the volume of material displaced, with JSC-1A having a higher range of slopes over which failures were observed than fine sand and coarse sand. Observations from these experiments may be useful to understand dendritic trough and furrow formation in regions of thin frost patches on Mars, such as on dune slopes and interdune material at the end of spring. However, sublimation was initiated by radiant heating with a heat lamp.

9. Other Radial Dendritic Features and Plumes in the Solar System

Through the study of araneiforms, we have learned a lot about sublimation processes under the low pressure regimes expected on other icy planetary surfaces - both applicable to araneiform analogs and the icy dynamics proposed to form them. Araneiforms are often referred to as "having no Earth analog," but they may serve as an analog for sublimation-driven activity elsewhere in the solar system. For example, an asterisk-shaped feature dubbed a "spider" by the Europa community was detected by the Galileo mission within Europa's Manannán crater (Moore et al., 2001) (Figure 17c). This feature has been compared to Martian araneiforms (Steinbrügge et al., 2020) and a connection was hypothesized regarding similar processes driven by pressure from beneath ice.

However, in this case, another dendritic feature on Earth may pose a suitable analog: "lake stars" are striking patterns (similar in shape to araneiforms), that develop on the surface of ice-covered lakes in winter (Knight, 1987) (Figures 17a and 17b). They form when a lake surface freezes and snowfall covers the thin ice, often developing into slush. Either due to the weight of the snow, or a protrusion such as a stick falling on the surface, the ice cracks and water wells through the snow or slush. This relatively warm water creates dark regions where it melts the snow. Locations with faster flow rates melt preferentially, leading to an instability that results in "fingers" (Knight, 1987; Tsai & Wettlaufer, 2007). Eventually, the water which has flowed through the system freezes, preserving this "star-like" pattern encased within the ice.

Recent work has used the formation of lake stars to understand the origin of the asterisk-shaped spider identified by the Galileo Mission in Europa's Manannán crater (L. Mc Keown et al., 2022). This work suggests that the feature may originate from a process similar to that forming lake stars on Earth, where its "arms" are not fractures but instead are low-albedo ice surrounded by frozen impact slurry. Experiments were performed with Europa granular ice simulant to explore the grain size and temperature ranges under which "lake star"-like patterns developed (Figures 17d and 17e). However, experiments under likely post-impact pressure ranges are needed to confirm whether similar patterns can form in ice under Europa conditions.

Distinct spacing and sizes are found within clusters of lake stars, qualitatively similar to the patterns seen with Martian spiders. Both sets of features, though forming via totally different processes, may display ordered distances between their centers due to diffusion through porous media (G. Portyankina et al., 2020) and a physical gradient—a pressure gradient or a thermal gradient for spiders and lake stars (Tsai & Wettlaufer, 2007), respectively. Diffusion models of Martian araneiforms (such as that described in Section 7.3) perhaps can be tuned to at least provide a rudimentary understanding of the formation of lake star patterns and spacing on Earth, and potentially then could be extrapolated to Europa. In turn, empirical field data on branching and spacing of lake stars on Earth combined with such models could be applied to morphometric studies of spiders on Mars. These connections provide an example of both the issue of equifinality in remote-observing icy planetary surfaces and the benefits of comparative planetology.

More examples of dendritic features may be found as more of the solar system is imaged at higher resolution. CO_2 ice is found broadly within the Solar System (described in detail in Ahrens et al. (2022)), from localized pockets within cold traps at the lunar poles (Schorghofer et al., 2021) to varying abundances across the Jovian satellites (e.g., G. B. Hansen and McCord, 2008; Hibbitts et al., 2003, 2000; McCord et al., 1998). However, sublimation timescales as

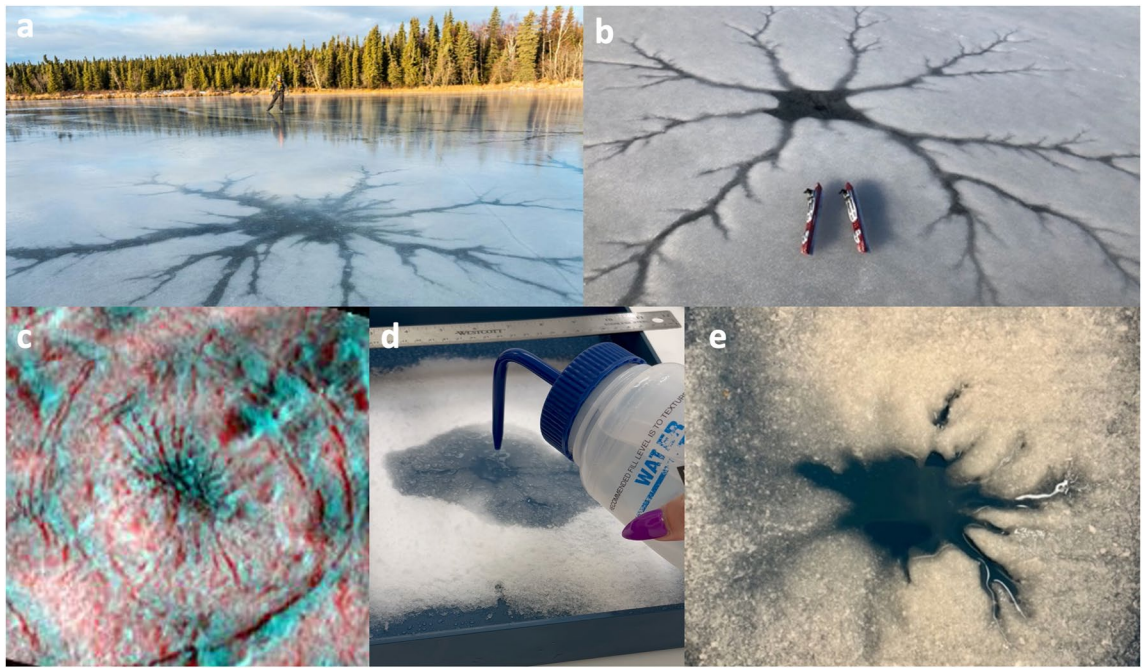

Figure 17. (a, b) Lake stars on Earth. Sources: Joe Stock (https://www.stockalpine.com/posts/swan-lake-ice-skate.html) and Jamie Hess (http://lakeice.squarespace.com/ice-stars/). (c) Asterisk–shaped "spider" feature on Europa's icy crust identified by the Galileo mission, proposed to have similar morphology and origin to a Terrestrial lake star. (d) Experiments under simulated post–impact temperature ranges to show lake–star patterns develop in Europa granular ice simulant. (e) An example of a dendritic "lake–star" pattern developed in the laboratory (L. Mc Keown et al., 2022).

well as substrate properties vary greatly among the distribution of CO_2 ices within the inner and outer Solar System and erosive substrate is unlikely on icy crusts. Moreover, the availability of CO_2 ice is not necessarily a precursor for the Solid State Greenhouse Effect or even sublimation plume activity. Furthermore, it also is possible for insolation-driven mobilization to occur for material *within* ices. The Kieffer Model was originally inspired by a modification of the conceptual model proposed to form the dark geyser-like eruptions observed by the Voyager 2 flyby of Neptune's moon, Triton in 1989 (Kirk et al., 1990; Soderblom et al., 1990) (Figure 18). This model suggested that nitrogen gas in a subsurface greenhouse environment pressurized by solar heating explosively vented to the surface, transporting plumes of ice and dark particles into the atmosphere. However, the likelihood of this hypothesis was recently called into question when additional analysis revealed that the ostensible relationship between the subsolar point and the locations of Triton's fans and plumes was not strong enough evidence for solar-driven geyser activity, citing cryovolcanism–driven origins as worthy of further investigation (Hofgartner et al., 2022).

How can the study of Martian araneiforms help to inform our understanding of analog features and processes on other planetary surfaces? A future Triton flyby mission could potentially distinguish between the solar-driven or cryovolcanic hypotheses. Remote-sensing observations by such a mission would benefit greatly from an understanding of the relationship between ice thickness, incident sun angle and geyser height/fan extent. High resolution, short temporal baseline change detection imaging of geyser activity on Mars combined with empirical data from laboratory experiments would help to inform this work. Furthermore, there may be many smaller, spider-like features on Europa and other ocean worlds that have shallow brine pools within their crusts. If we detect such features, we will be equipped with both decades of data on Martian araneiforms and models describing how similar geomorphological patterns could form in different environments.

10. Open Questions and Future Work Needed

As discussed throughout this paper, there are many open questions promoting areas for future work on araneiforms and the process thought to form them. Below, we provide starting thoughts on areas that merit further investigation, as well as methods that would help to address them.

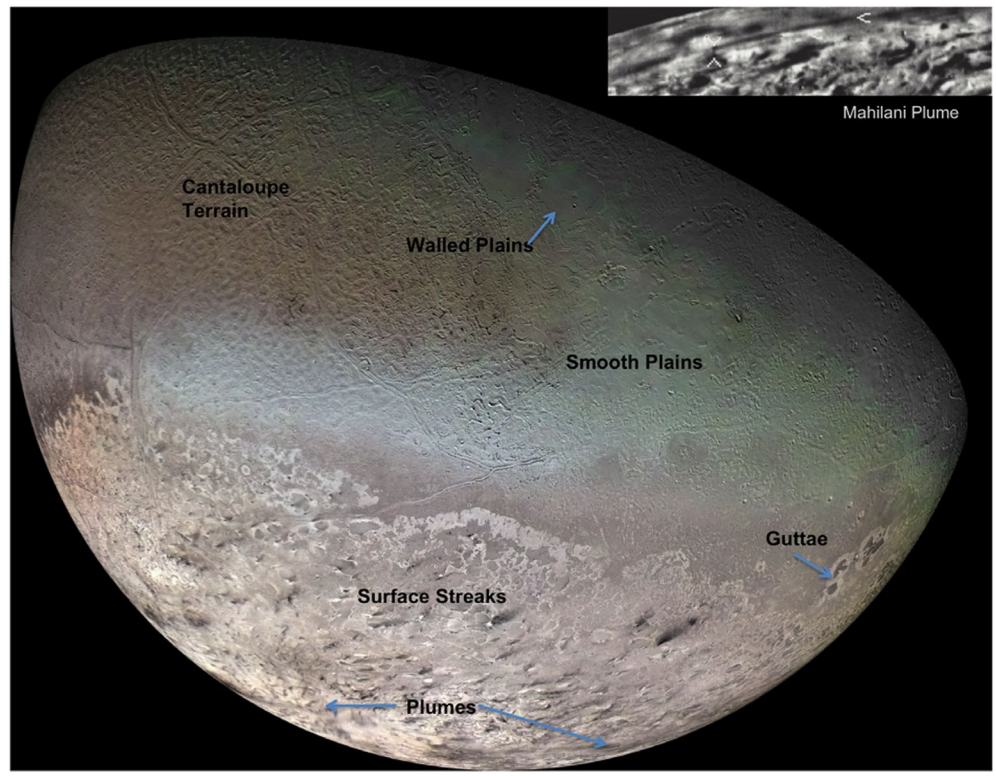

Figure 18. Plumes on Triton (C. J. Hansen et al., 2021). These were originally postulated to be formed by the Solid State Greenhouse Effect similar to that forming araneiforms on Mars, but within Nitrogen ice. However, variants on that hypothesis have recently been called into question (Hofgartner et al., 2022), and a deeper consideration of a cryovolcanic origin has been encouraged.

10.1. Ice Properties—Providing Context for the Kieffer Model

1. How does ice type, thickness and H_2O content affect basal sublimation efficacy?
2. How does the timing and timescales of ice residency and sublimation affect araneiform formation?
3. How does dust within, on top of and below the seasonal ice layer affect araneiform formation?

As outlined in Sections 1.1 and 7, the thickness, strength, and purity of the ice will influence the sublimation rate at the base of the ice and buildup of gas, and hence the extent to which the Kieffer model cryojetting process can operate. Thus, estimates on the timing and seasonal timescales of ice "residency" and sublimation are important inputs for models that create basal pressure. Such information could be acquired through mapping the different seasonal ice parameters present on Mars as a function of time of year and latitude/location—for example, ice overburden thicknesses, mixture amount and structure of water (Andrieu et al., 2018) and CO_2 ice as well as dust in the ice, timing of deposition and sublimation, and fracture density within early spring slab ice. While TES emissivity data have been used to constrain ice sintering timescales on the order of sols (?Cornwall & Titus, 2010), laboratory experiments are also needed to constrain timescales of ice grain sintering under temperature and pressure regimes reflective of different araneiform locations, and the influence of dust within, on top of and below the ice on ice structure evolution and sublimation. Finally, modeling and laboratory experiments would help constrain how plume height and velocity is influenced by these same environmental parameters.

10.2. Local Geologic Properties—Providing Context for the Kieffer Model

1. Do araneiform locations also represent the thickness of the fines on which they are superposed?
2. Does grain size and porosity/permeability of fines vary within the SPLD?
3. What is the cutoff point for grain size and consolidation wherein spiders can form?

As discussed in Sections 1.1, 4.2, and 5, the formation of araneiforms and their distinct morphologies are proposed to be driven by the properties of the material upon which they are eroded. In turn, knowing more about this relationship could allow us to identify surface properties within araneiform locations. For example, if ground ice were closer to the surface (with a thin layer of fines between it and the seasonal ice layer), this may result in a lower thermal gradient within the layer of mobilized regolith during basal sublimation and potentially less vigorous sublimation, resulting in shallower, less dendritic araneiforms. Additionally, the very distinct clusters of spiders with non-random spacing may be reflective of varying grain size, porosity and permeability of their local regolith material. Experiments of the Kieffer model exploring the feedback between such parameters and araneiform morphology and activity, as well as neutron spectrometer mapping within the south polar regions could help to put limits on the ranges of ice types and thickness that will instigate basal sublimation that will have geomorphic agency.

10.3. Broad Geologic Properties—Providing Validation for the Kieffer Model

1. How do the timing, extent and placement of the cryptic region relate to spider formation?
2. Why do spiders and dendritic troughs develop in the SH but not in the NH?
3. How do spiders relate spatially and morphologically to sequestered ice, the cryptic region and the SPRC?

As described in Sections 1.1 and 4, the spatial connection between spiders and cryptic terrain suggests that the formation of the translucent CO_2 ice is a control on araneiform generation. However, whether completely translucent ice truly is necessary for araneiform formation remains an open question. More data in general are needed on the conditions for translucent ice formation–whether directly condensed or sintered through the winter. High resolution surface roughness maps could also provide insight into whether the cryptic region is more susceptible to cracking due to small-scale topography.

Second, while various hypotheses have been offered (Section 1.1.2) and observations and models have indicated that topographical climate forcing may be key (Colaprete et al., 2005), the basis for the geographical distribution of the cryptic region has not been fully elucidated, as well as why this region of translucent slab ice reappears in the same location annually. Potentially, the presence of spiders may cause points of topographic weakness and thus cause repeats in cracking locations and dust cycling from within the spider troughs. However, even if true, this does not explain why spiders formed in this location to begin with.

Additionally, with improved spatial resolution and coverage since spiders were first mapped, more spiders and dendritic features have been found beyond the cryptic region. Does this imply that the cryptic region may have been more expansive or occurred at a different location during past climates?

Finally, mapping of spiders is currently an indicative of a high concentration of spiders close to the SPRC, where there should be ground ice within the top few cm. If this regolith is indurated, it is possible that spiders may have formed (and be forming) at very, very slow rates via repeated scouring events. Away from the edge of the perennial cap, water would diffuse into the atmosphere, making the regolith looser and more desiccated, so perhaps spiders at lower latitudes could have formed at faster rates. Contiguous mapping of spiders and their relative stratigraphy is needed to investigate whether spiders over a broad geological context in the south polar regions have different morphologies and to test if these features may have formed over different timescales. Complementary lab experiments of spider formation could elucidate the conditions that may be reflective of those morphologies, perhaps linking them to specific present or past climates.

10.4. Past Context—Extrapolation of the Kieffer Model for Interpretation of Morphology

1. Did conditions favorable to spider formation occur over one or few efficient erosional events in a past climate, or do the features we see today represent 1,000+ years of very slow erosion rates? Are spiders outside of the current-day "cryptic region" relicts from a past climate wherein the cryptic region was more expansive or existed within a different location of the seasonal ice cap?
2. How extensive and thick was the seasonal CO_2 ice layer in the past?
3. What is the lateral variability of depth to the water ice table and does this have a relationship with spider locations and patterned ground?

It is unclear how diffuse or vigorous present-day sublimation is relative to sublimation rates under past climates. Given the number of physical factors that may influence araneiform formation (e.g., ice thickness, ice type, sediment consolidation, dust presence etc.), there is likely an ideal condition under which cryo-jetting is most effective at eroding the surface. Spiders surrounding the south polar cap have not yet been observed to newly form or extend today, despite extensive monitoring. This raises the important question: in the past, were conditions more conducive to spider formation and sublimation being more energetic? While numerical modeling of past climate regimes has been explored, modeling of past *seasonal* dynamics, particularly with respect to the extent and thickness of the seasonal ice layer, is needed. Studying araneiform morphologies and their relative stratigraphy with respect to recent geological landforms may unlock information on the environmental conditions under which they formed. Combined with empirical data collected from laboratory experiments probing these physical parameters, such an approach may in turn helping us to understand how seasonal change modified the Martian surface during paleoclimates. Future ground truthing would be greatly beneficial in dating the variety of terrains on which araneiforms are found and constraining the present and past depth to water ice.

10.5. Jetting/Blotches/Fans Process—Additional Parts of the Kieffer Model

1. How often does jetting activity occur, and over what duration?
2. Over what basal area will a vent relieve pressure, thus setting a minimum spacing between jets and araneiforms?
3. Is earlier fan/spot activity more likely to lead to araneiform formation?
4. How is the spatial extent of blotches and fans controlled by measurable characteristics of the spewed material and of the ice?
5. What are the white fans made of?

Despite imaging campaigns over the last decade, no active jets have yet been identified in remote imagery (C. J. Hansen et al., 2020). Thus, questions about the timing, duration, and rates of jetting activity, especially the activity that may lead to araneiforms, can only be hypothesized at this time and explored with theoretical models. A more easily identified and measured feature known to be related to the jetting are the blotches and fans left behind as sediment is carried by the jet and deposited onto the frost layer. Thus, being able to connect the morphometrics, orientations, and appearance of these features to the jetting dynamics, via laboratory experiments and models, is key to providing "ground truth" constraints. In those studies, both ice characteristics, such as its level of translucency, and grain characteristics are likely to control the final extent and shape of the fans and blotches—thus providing a way to predict which types of ice and substrate, along with the timing of sublimation, are more likely to generate araneiforms. These predictions, when compared with maps of substrate type and seasonal ice formation (in the present or under past climate conditions) as well as maps of where types of araneiforms or sublimation markers are found, yield a robust way to test the details of the Kieffer Model.

10.6. Araneiform Morphology and Activity

1. How old are spiders and are they presently active? Is it possible for large spiders to grow over just one or a few efficient erosion events? Will the presently observed dendritic troughs eventually grow into spider scales?
2. How do specific surface topography and substrate and ice characteristics control the different spider morphologies?
3. For spider clusters, to what degree do vent spacing and sediment properties influence their very distinct spacing and level of branching?

As discussed in Sections 4 and 5, activity and morphology are the two main factors that differentiate spiders from furrows and dendritic troughs. One significant unanswered question is whether spiders are growing at a much slower rate than dendritic troughs and furrows, due to sediment mobility differences, or if they are dormant/relict features that once grew when conditions were more favorable. This question feeds into further thoughts regarding the different individual morphologies of spiders and what can be interpreted from specific morphometrics: were some more evolved and entangled spiders once less dendritic and expansive in nature? Did these types grow over many venting episodes and thus, are they much older than less tortuous types? For example, were "thin" spider morphologies more similar to "fat," or do "baby" spiders represent spiders in their very early stages of growth?

One possible way to understand the growth rate of spiders is to extrapolate present-day change detection of dendritic troughs to the scale of spiders, as was done by G. Portyankina et al. (2017). However, ice thicknesses, grain size and possibly sediment mobility and ice type differ between spider and dendritic trough environments,

and we do not have a strong enough knowledge of small-scale ice types and thicknesses on Mars - especially toward the midlatitudes, where furrows and dendritic troughs are located.

To better understand the distinct "classes" of spiders and why certain spiders "cluster" or "taper off" into different morphologies, a more contiguous map showing the locations of spider types is needed. This map should then be combined with maps of frost type and thickness, as well as local geological characterizations relevant to spider formation (see Sections 1.2 and 4.2). For example, is there a difference in spider morphologies found on and off the SPLD, or within and outside the cryptic region? Additionally, the influence of the following parameters on morphology should be explored empirically: dust, ice thickness, sediment consolidation, grain size distribution, the extent and residency timescale of the seasonal cap, insolation angle and flux, slope, surface roughness, ice type, fracture density of overlying ice, and pressure and temperature conditions (complementing investigations outlined in Sections 2–10.2). Knowing how each of these factors control morphology would enable the identification of substrate and ice properties on Mars based on araneiform morphology. A further step would be to investigate how many of these parameters may have varied with changing obliquity with numerical modeling; this may tie certain morphologies to past conditions. Lastly, while initial steps have been taken to model araneiform morphologies, a semi-analytical model of araneiform formation, inputting empirical parameters taken from laboratory experiments, would be very beneficial to better understanding their formative environments on Mars.

10.7. Araneiforms and Their Context in the Solar System

1. Are there dendritic features on other planetary bodies where basal sublimation may occur under surface ice? What are the dendritic features that have not formed through a Kieffer model-type system?
2. How can we extrapolate from observations or models of jet activity on Mars so as to understand potential non-cryovolcanic plumes and fans in the outer solar system?

To date, dendritic features have been observed on Earth, Mars, and Europa (as described in Section 9). As better cameras are sent to more bodies, comparative planetology with the Martian features is likely to be critical in prompting new hypotheses or providing quantitative guidance to describe the features and discriminate between formation models. As discussed in Section 9, despite differing formation processes, the formation of other dendritic features can be informed by our knowledge of Martian araneiforms, which benefits from repeat high-resolution monitoring of the Martian formation and activity. A similar approach can be applied to understanding non-cryovolcanic plumes and fans in the outer solar system, based on studies of Martian jets and the Kieffer model.

While many landforms on Mars have benefited from our ground-truth knowledge of analogs on Earth, our understanding of features like araneiforms, which have no direct Earth analog, has benefited from conceptual modeling and testing of those models with laboratory experiments and numerical models. With the upcoming Europa Clipper mission to Jupiter's moon Europa, we are likely to detect even more surface expressions that have no direct Earth analogs. We need to be equipped to understand them and the potential they hold to indicate environmental conditions.

11. Conclusion

Martian araneiforms provide a record of a geomorphic process that is completely different from terrestrial processes, and yet exhibit a morphology found in many terrestrial natural systems. This both hints at the equifinality of diffusion-limited processes that may be found throughout the solar system, and also provided a starting point for the development of the Kieffer model, which has been instrumental in elucidating some very un-Earth-like aspects of the Martian climate. Furthermore, the distinct morphometrics and patterns of furrows, dendritic troughs, and many types of spider hints at information encoded into these features about environmental controls for the geomorphic activity, including specific seasonal frost conditions. Some of these features may even encode information about past, different climates, enabling a quantitative understanding of how the seasonal frost distribution has changed through recent martian history.

As outlined in this review, the multipronged approach of numerical modeling, laboratory experiments, and spacecraft observation analysis/mapping has (and will continue to) advance our understanding of these extraterrestrial features and ability to interpret them as records of subsurface and surface properties and seasonal frost grain

characteristics and layer strength. The main major questions now focus on information needed to refine the Kieffer model and to validate its expression over broader scales. Furthermore, as the Kieffer model and investigations of araneiforms have matured, we are becoming more able to use these martian features as a starting point to investigate dendritic geomorphic features found on other planetary bodies (even if formed through different processes), starting with (but not limited to) the feature in Manannán crater on Europa, as well as potential basal sublimation-driven jetting. The studies of araneiforms provide an example of the many branched studies and insights that come from the investigation of intriguing surface features, as we become able to quantitatively connect the morphologies of such features to past and present dynamic processes and formation/evolution conditions.

Data Availability Statement

The data discussed in this review paper are available from the cited manuscripts. HiRISE images are openly available (McEwen, 2007). The data presented in L. Mc Keown et al. (2023b) are openly available at L. Mc Keown et al. (2023a).

Acknowledgments
The research was carried out at the Jet Propulsion Laboratory, California Institute of Technology, under a contract with the National Aeronautics and Space Administration (80NM0018D0004). L.E.M., J.E.C., and S.D. were funded by the NASA Mars Data Analysis Program (award no. 80NM0018F0719) at the Jet Propulsion Laboratory. S.P. was supported by the NASA Mars Data Analysis Program (20-MDAP20_2–0024). G.P., K.-M.A. and C.J.H. were supported by NASA Grant 80NSSC20K0748. The authors would like to sincerely thank the reviewers, Dr. Tim Titus and Dr. Fréderic Schmidt, for their expertise and very helpful comments, which have greatly benefited the paper.

References

Aharonson, O. (2004). Sublimation at the base of a seasonal CO_2 slab on Mars. In *35th annual lunar and planetary science conference*.

Aharonson, O., Zuber, M. T., Smith, D. E., Neumann, G. A., Feldman, W. C., & Prettyman, T. H. (2004). Depth, distribution, and density of CO_2 deposition on Mars. *Journal of Geophysical Research: Planets*, *109*(E5), E05004. https://doi.org/10.1029/2003je002223

Ahrens, C., Meraviglia, H., & Bennett, C. (2022). A geoscientific review on co and CO_2 ices in the outer solar system. *Geosciences*, *12*(2), 51. https://doi.org/10.3390/geosciences12020051

Andrieu, F., Schmidt, F., Douté, S., & Chassefière, E. (2018). Albedo control of seasonal south polar cap recession on Mars. *Icarus*, *315*, 158–173. https://doi.org/10.1016/j.icarus.2018.06.019

Attree, N., Kaufmann, E., & Hagermann, A. (2021). Gas flow in martian spider formation. *Icarus*, *359*, 114355. https://doi.org/10.1016/j.icarus.2021.114355

Aye, K.-M., Portyankina, G., & Thomas, N. (2010). Semi-automatic measures of activity in the Inca city region of Mars using morphological image analysis. In *Lunar and planetary science conference* (Vol. 41, p. 2707).

Aye, K. M., Schwamb, M. E., Portyankina, G., Hansen, C. J., McMaster, A., Miller, G. R., et al. (2019). Planet four: Probing springtime winds on Mars by mapping the southern polar CO_2 jet deposits. *Icarus*, *319*, 558–598. https://doi.org/10.1016/j.icarus.2018.08.018

Balme, M., Gallagher, C., & Hauber, E. (2013). Morphological evidence for geologically young thaw of ice on Mars: A review of recent studies using high-resolution imaging data. *Progress in Physical Geography: Earth and Environment*, *37*(3), 289–324. https://doi.org/10.1177/0309133313477123

Bandfield, J. L., & Feldman, W. C. (2008). Martian high latitude permafrost depth and surface cover thermal inertia distributions. *Journal of Geophysical Research*, *113*(E8), E08001. https://doi.org/10.1029/2007JE003007

Bapst, J., Byrne, S., Bandfield, J. L., & Hayne, P. O. (2019). Thermophysical properties of the north polar residual cap using Mars global surveyor thermal emission spectrometer. *Journal of Geophysical Research: Planets*, *124*(5), 1315–1330. https://doi.org/10.1029/2018JE005786

Bibring, J. P., Langevin, Y., Poulet, F., Gendrin, A., Gondet, B., Berthe, M., et al. (2004). Perennial water ice identified in the south polar cap of Mars. *Nature*, *428*(6983), 627–630. https://doi.org/10.1038/nature02461

Bierson, C. J., Phillips, R. J., Smith, I. B., Wood, S. E., Putzig, N. E., Nunes, D., & Byrne, S. (2016). Stratigraphy and evolution of the buried CO_2 deposit in the Martian south polar cap. *Geophysical Research Letters*, *43*(9), 4172–4179. https://doi.org/10.1002/2016GL068457

Blackburn, D. G., Bryson, K. L., Chevrier, V. F., Roe, L. A., & White, K. F. (2010). Sublimation kinetics of CO_2 ice on Mars. *Planetary and Space Science*, *58*(5), 780–791. https://doi.org/10.1016/j.pss.2009.12.004

Bourke, M., & McGaley-Towle, Z. (2014). Why do sand furrow distributions vary in the North Polar latitudes on Mars? In *EGU general assembly conference abstracts* (Vol. 16, p. 13626)

Bourke, M. C. (2013). The formation of sand furrows by cryo-venting on Martian dunes. In *Lunar and planetary science conference* (Vol. 44, p. 2919)

Bourke, M. C., & Cranford, A. (2011). Seasonal furrow formation on Mars polar dunes. In *Fifth international conference on mars polar science and exploration* (Vol. 1623, p. 6059)

Bowie, D. (1972). The rise and fall of ziggy stardust and the spiders from mars—Wikipedia, the free encyclopedia. Retrieved from http://en.wikipedia.org/w/index.php?title=The%20Rise%20and%20Fall%20of%20Ziggy%20Stardust%20and%20the%20Spiders%20from%20Mars&oldid=1114135125

Boynton, W. V., Feldman, W. C., Squyres, S. W., Prettyman, T. H., Brückner, J., Evans, L. G., et al. (2002). Distribution of hydrogen in the near surface of Mars: Evidence for subsurface ice deposits. *Science*, *297*(5578), 81–85. https://doi.org/10.1126/science.1073722

Bramson, A. M., Byrne, S., & Bapst, J. (2017). Preservation of midlatitude ice sheets on Mars. *Journal of Geophysical Research: Planets*, *122*(11), 2250–2266. https://doi.org/10.1002/2017JE005357

Brown, R. H., Kirk, R. L., Johnson, T. V., & Soderblom, L. A. (1990). Energy sources for triton's geyser-like plumes. *Science*, *250*(4979), 431–435. https://doi.org/10.1126/science.250.4979.431

Buhler, P. B., Ingersoll, A. P., Piqueux, S., Ehlmann, B. L., & Hayne, P. O. (2020). Coevolution of Mars' atmosphere and massive south polar CO_2 ice deposit. *Nature Astronomy*, *4*, 364–371. https://doi.org/10.1038/s41550-019-0976-8

Bunde, A., & Havlin, S. (1996). *Fractals and disordered systems*. Springer-Verlag.

Byrne, S. (2009). The polar deposits of Mars. *Annual Review of Earth and Planetary Sciences*, *37*(1), 535–560. https://doi.org/10.1146/annurev.earth.031208.100101

Byrne, S., & Ingersoll, A. (2003). A sublimation model for Martian south polar ice features. *Science*, *299*(5609), 1051–1053. https://doi.org/10.1126/science.1080148

Calvin, W. M., Cantor, B., & James, P. (2017). Interannual and seasonal changes in the south seasonal polar cap of Mars: Observations from MY 28–31 using marci. *Icarus*, *292*, 144–153. https://doi.org/10.1016/j.icarus.2017.01.010

Calvin, W. M., James, P. B., Cantor, B. A., & Dixon, E. M. (2015). Interannual and seasonal changes in the north polar ice deposits of Mars: Observations from MY 29–31 using MARCI. *Icarus*, *251*, 181–190. https://doi.org/10.1016/j.icarus.2014.08.026

Calvin, W. M., & Seelos, K. D. (2019). Evolution within the martian southern seasonal cryptic terrain from CTX and CRISM. In *2019 AGU fall meeting* (p. P33F-3501)

Cantor, B., Malin, M., & Edgett, K. S. (2002). Multiyear Mars orbiter camera (moc) observations of repeated Martian weather phenomena during the northern summer season. *Journal of Geophysical Research*, *107*(E3), 3-1–3-8. https://doi.org/10.1029/2001JE001588

Cesar, C., Pommerol, A., Thomas, N., Portyankina, G., Hansen, C. J., Tornabene, L. L., et al. (2022). Seasonal southern circum-polar spots and araneiforms observed with the colour and stereo surace imaging system (CaSSIS). *Planetary and Space Science*, *224*, 105593. https://doi.org/10.1016/j.pss.2022.105593

Chinnery, H. E., Hagermann, A., Kaufmann, E., & Lewis, S. R. (2019). The penetration of solar radiation into carbon dioxide ice. *Journal of Geophysical Research: Planets*, *123*(4), 864–871. https://doi.org/10.1002/2018je005539

Chinnery, H. E., Hagermann, A., Kaufmann, E., & Lewis, S. R. (2020). The penetration of solar radiation into granular carbon dioxide and water ices of varying grain sizes on Mars. *Journal of Geophysical Research: Planets*, *125*(4), e2019JE006097. https://doi.org/10.1029/2019JE006097

Colaprete, A., Barnes, J. R., Haberle, R. M., Hollingsworth, J. L., Kieffer, H. H., & Titus, T. N. (2005). Albedo of the south pole on Mars determined by topographic forcing of atmosphere dynamics. *Nature*, *435*(7039), 184–188. https://doi.org/10.1038/nature03561

Cornwall, C., & Titus, T. N. (2010). A comparison of Martian north and south polar cold spots and the long-term effects of the 2001 global dust storm. *Journal of Geophysical Research*, *115*(E6), E06011. https://doi.org/10.1029/2009JE003514

de Villiers, S., Nermoen, A., Jamtveit, B., Mathiesen, J., Meakin, P., & Werner, S. C. (2012). Formation of Martian araneiforms by gas-driven erosion of granular material. *Geophysical Research Letters*, *39*(13), L13204. https://doi.org/10.1029/2012gl052226

Dickson, J. L., Ehlmann, B. L., Kerber, L., Fassett, C. I., Hare, T. M., Quinn, D. P., et al. (2020). The global CTX mosaic of Mars: Lessons for the construction and dissemination of massive imaging data sets. In *51st annual lunar and planetary science conference* (p. 2309)

Diniega, S., Bramson, A., Buratti, B., Buhler, P., Burr, D., Chojnacki, M., et al. (2021). Modern Mars' geomorphological activity, driven by wind, frost, and gravity. *Geomorphology*, *380*, 107627. https://doi.org/10.1016/j.geomorph.2021.107627

Diniega, S., Hansen, C. J., Allen, A., Grigsby, N., Li, Z., Perez, T., & Chojnacki, M. (2019). Dune-slope activity due to frost and wind throughout the north polar erg, Mars. In *Martian Gullies and their Earth analogues* (p. 467). Geological Society, London, Special Publication. https://doi.org/10.1144/SP467.6

Diniega, S., Hansen, C. J., McElwaine, J. N., Hugenholtz, C. H., Dundas, C. M., McEwen, A. S., & Bourke, M. C. (2013). A new dry hypothesis for the formation of Martian linear gullies. *Icarus*, *225*(1), 526–537. https://doi.org/10.1016/j.icarus.2013.04.006

Ditteon, R., & Kieffer, H. H. (1979). Optical properties of solid CO_2: Application to Mars. *Journal of Geophysical Research*, *84*(B14), 8294–8300. https://doi.org/10.1029/JB084iB14p08294

Dundas, C. M., Diniega, S., Hansen, C. J., Byrne, S., & McEwen, A. S. (2012). Seasonal activity and morphological changes in Martian gullies. *Icarus*, *220*(1), 124–143. https://doi.org/10.1016/j.icarus.2012.04.005

Durham, W. B., Kirby, S. H., & Stern, L. A. (1998). Rheology of planetary ices. In B. Schmitt, C. Bergh, & M. Festou (Eds.), *Solar system ices, based on reviews presented at the international symposium "solar system ices" held in Toulouse, France, on March 27–30, 1995* (pp. 63–78). https://doi.org/10.1007/978-94-011-5252-5_3

Forget, F., Byrne, S., Head, J., Mischna, M., & Schörghofer, N. (2017). Recent climate variations. In R. M. Haberle, R. T. Clancy, F. Forget, M. D. Smith, & R. W. Zurek (Eds.), *The atmosphere and climate of Mars* (pp. 497–525). Cambridge University Press.

Forget, F., & Pollack, J. B. (1996). Thermal infrared observations of the condensing Martian polar caps: CO_2 ice temperatures and radiative budget. *Journal of Geophysical Research*, *101*(E7), 16865–16879. https://doi.org/10.1029/96je01077

Gardin, E., Allemand, P., Quantin, C., & Thollot, P. (2010). Defrosting, dark flow features, and dune activity on Mars: Example in Russell crater. *Journal of Geophysical Research*, *115*(E6), E06016. https://doi.org/10.1029/2009JE003515

Gary-Bicas, C. E., Hayne, P. O., Horvath, T., Heavens, N. G., Kass, D. M., Kleinböhl, A., et al. (2020). Asymmetries in snowfall, emissivity, and albedo of Mars' seasonal polar caps: Mars climate sounder observations. *Journal of Geophysical Research: Planets*, *125*(5), e2019JE006150. https://doi.org/10.1029/2019JE006150

Greeley, R., Lancaster, N., Lee, S., & Thomas, P. (1992). Martian aeolian processes, sediments, and features. In M. George (Ed.), *Mars* (pp. 730–766).

Green, J. (2001). The extraterrestrial materials simulation laboratory.

Grima, C., Kofman, W., Mouginot, J., Phillips, R. J., Hérique, A., Biccari, D., et al. (2009). North polar deposits of Mars: Extreme purity of the water ice. *Geophysical Research Letters*, *36*(3), L03203. https://doi.org/10.1029/2008GL036326

Hansen, C. J., Bourke, M., Bridges, N., Byrne, S., Colón, C., Diniega, S., et al. (2011). Seasonal erosion and restoration of Mars' northern polar dunes. *Science*, *331 6017*, 575–578. https://doi.org/10.1126/science.1197636

Hansen, C. J., Byrne, S., Portyankina, G., Bourke, M., Dundas, C., McEwen, A., et al. (2013). Observations of the northern seasonal polar cap on Mars: I. Spring sublimation activity and processes. *Icarus*, *225*(2), 881–897. https://doi.org/10.1016/j.icarus.2012.09.024

Hansen, C. J., Conway, S., Portyankina, G., Thomas, N., & McEwen, A. S. (2020). Searching for seasonal jets on Mars in CaSSIS and HiRISE images. In *51st annual lunar and planetary science conference* (p. 2351)

Hansen, C. J., Grundy, W., Hofgartner, J., Martin, E., Mitchell, K., Nimmo, F., et al. (2021). Triton: Fascinating moon, likely ocean world, compelling destination!. *Bulletin of the American Astronomical Society*, *53*(4), 184. https://doi.org/10.3847/25c2cfeb.55e7710d

Hansen, C. J., Thomas, N., Portyankina, G., McEwen, A., Becker, T., Byrne, S., et al. (2010). HiRISE observations of gas sublimation-driven activity in Mars' southern polar regions: I. Erosion of the surface. *Icarus*, *205*(1), 283–295. https://doi.org/10.1016/j.icarus.2009.07.021

Hansen, G. B. (1997). The infrared absorption spectrum of carbon dioxide ice from 1.8 to 333 μm. *Journal of Geophysical Research E: Planets*, *102*(E9), 21569–21587. https://doi.org/10.1029/97JE01875

Hansen, G. B. (2005). Ultraviolet to near-infrared absorption spectrum of carbon dioxide ice from 0.174 to 1.8 μm. *Journal of Geophysical Research*, *110*(E11), E11003. https://doi.org/10.1029/2005JE002531

Hansen, G. B., & McCord, T. B. (2008). Widespread CO_2 and other non-ice compounds on the anti-Jovian and trailing sides of Europa from Galileo/NIMS observations. *Geophysical Research Letters*, *35*(1), L01202. https://doi.org/10.1029/2007GL031748

Hao, J., Michael, G., Adeli, S., Jaumann, R., Portyankina, G., Hauber, E., et al. (2020). Variability of spider spatial configuration at the Martian south pole. *Planetary and Space Science*, *185*, 104848. https://doi.org/10.1016/j.pss.2020.104848

Hao, J., Michael, G. G., Adeli, S., & Jaumann, R. (2019). Araneiform terrain formation in Angustus Labyrinthus, Mars. *Icarus*, *317*, 479–490. https://doi.org/10.1016/j.icarus.2018.07.026

Hayne, P. O., Paige, D. A., & Heavens, N. G. (2014). The role of snowfall in forming the seasonal ice caps of Mars: Models and constraints from the Mars Climate Sounder. *Icarus*, *231*, 122–130. https://doi.org/10.1016/j.icarus.2013.10.020

Hayne, P. O., Paige, D. A., Schofield, J. T., Kass, D. M., Kleinböhl, A., Heavens, N. G., & McCleese, D. J. (2012). Carbon dioxide snow clouds on Mars: Southern polar winter observations by the Mars climate sounder. *Journal of Geophysical Research*, *117*(E8), E08014. https://doi.org/10.1029/2011JE004040

Hess, S., Henry, R. M., & Tillman, J. E. (1979). The seasonal variation of atmospheric pressure on Mars as affected by the south polar cap. *Journal of Geophysical Research*, *84*(B6), 2923–2927. https://doi.org/10.1029/jb084ib06p02923

Hibbitts, C. A., McCord, T. B., & Hansen, G. B. (2000). Distributions of CO_2 and SO_2 on the surface of callisto. *Journal of Geophysical Research*, *105*(E9), 22541–22557. https://doi.org/10.1029/1999JE001101

Hibbitts, C. A., Pappalardo, R. T., Hansen, G. B., & McCord, T. B. (2003). Carbon dioxide on ganymede. *Journal of Geophysical Research*, *108*(E5), 5036. https://doi.org/10.1029/2002JE001956

Hofgartner, J. D., Birch, S. P., Castillo, J., Grundy, W. M., Hansen, C. J., Hayes, A. G., et al. (2022). Hypotheses for triton's plumes: New analyses and future remote sensing tests. *Icarus*, *375*, 114835. https://doi.org/10.1016/j.icarus.2021.114835

Holstein-Rathlou, C., Merrison, J., Iversen, J. J., Jakobsen, A., Nicolajsen, R., Nurnberg, P., et al. (2014). An environmental wind tunnel facility for testing meteorological sensor systems. *Journal of Atmospheric and Oceanic Technology*, *31*(2), 447–457. https://doi.org/10.1175/JTECH-D-13-00141.1

Horsfield, K. (1976). Some mathematical properties of branching trees with application to the respiratory system. *Bulletin of Mathematical Biology*, *38*(3), 305–315. https://doi.org/10.1016/S0092-8240(76)80055-9

Horton, R. (1945). Erosional development of streams and their drainage basins; hydrophysical approach to quantitative morphology. *GSA Bulletin*, *56*(3), 275–370. https://doi.org/10.1130/0016-7606(1945)56[275:EDOSAT]2.0.CO;2

Houben, H., Haberle, R. M., Young, R. E., & Zent, A. P. (1997). Modeling the Martian seasonal water cycle. *Journal of Geophysical Research*, *102*(E4), 9069–9083. https://doi.org/10.1029/97je00046

Hvidberg, C., Fishbaugh, K., Winstrup, M., Svensson, A., Byrne, S., & Herkenhoff, K. E. (2012). Reading the climate record of the Martian polar layered deposits. *Icarus*, *221*(1), 405–419. https://doi.org/10.1016/j.icarus.2012.08.009

Ingersoll, A. (1970). Mars: Occurrence of liquid water. *Science*, *168*(3934), 972–973. https://doi.org/10.1126/science.168.3934.972

Jakosky, B. M., Mellon, M. T., Varnes, E. S., Feldman, W. C., Boynton, W. V., & Haberle, R. M. (2005). Mars low-latitude neutron distribution: Possible remnant near-surface water ice and a mechanism for its recent emplacement. *Icarus*, *175*(1), 58–67. https://doi.org/10.1016/j.icarus.2004.11.014

James, P. B., Kieffer, H. H., & Paige, D. A. (1992). The seasonal cycle of carbon dioxide on Mars. In *Mars* (pp. 934–968).

Kaufmann, E., Attree, N., Bradwell, T., & Hagermann, A. (2020). Hardness and yield strength of co ice under martian temperature conditions. *Journal of Geophysical Research: Planets*, *125*(3), e2019JE006217. https://doi.org/10.1029/2019JE006217

Kaufmann, E., & Hagermann, A. (2017). Experimental investigation of insolation-driven dust ejection from Mars' CO_2 ice caps. *Icarus*, *282*, 118–126. https://doi.org/10.1016/j.icarus.2016.09.039

Kaufmann, E., Koemle, N., & Kargl, G. (2006). Laboratory simulation experiments on the solid-state greenhouse effect in planetary ices. *Icarus*, *185*(1), 274–286. https://doi.org/10.1016/j.icarus.2006.07.009

Kelly, N. J., Boynton, W. V., Kerry, K. E., Hamara, D., Janes, D. M., Reddy, R. C., et al. (2006). Seasonal polar carbon dioxide frost on Mars: CO_2 mass and columnar thickness distribution. *Journal of Geophysical Research*, *111*(E3), E03S07. https://doi.org/10.1029/2006JE002678

Khuller, A., Christensen, P., Harrison, T., & Diniega, S. (2021). The distribution of frosts on Mars: Links to present-day gully activity. *Journal of Geophysical Research: Planets*, *126*(3), e2020JE006577. https://doi.org/10.1029/2020JE006577

Kieffer, H. H. (1968). *Near infrared spectral reflectance of simulated Martian frosts* (Doctoral dissertation). California Institute of Technology. Retrieved from https://thesis.library.caltech.edu/2906/

Kieffer, H. H. (1970). Spectral reflectance of CO_2-H_2O frosts. *Journal of Geophysical Research*, *75*(3), 501–509. https://doi.org/10.1029/JC075i003p00501

Kieffer, H. H. (2000). Annual punctuated CO_2 slab-ice and jets on Mars. In *Second international conference on mars polar science and exploration* (p. 93)

Kieffer, H. H. (2003). Behavior of solid CO_2 on Mars: A real zoo. In A. L. Albee & H. H. Kieffer (Eds.), *Sixth international conference on mars* (p. 3158)

Kieffer, H. H. (2007). Cold jets in the Martian polar caps. *Journal of Geophysical Research*, *112*(E8), E08005. https://doi.org/10.1029/2006je002816

Kieffer, H. H., Christensen, P. R., & Titus, T. N. (2006). CO_2 jets formed by sublimation beneath translucent slab ice in Mars' seasonal south polar ice cap. *Nature*, *442*(7104), 793–796. https://doi.org/10.1038/nature04945

Kieffer, H. H., Titus, T. N., Mullins, K. F., & Christensen, P. R. (2000). Mars south polar spring and summer behavior observed by tes: Seasonal cap evolution controlled by frost grain size. *Journal of Geophysical Research*, *105*(E4), 9653–9699. https://doi.org/10.1029/1999JE001136

Kirk, R. L., Brown, R. H., & Soderblom, L. A. (1990). Subsurface energy storage and transport for solar-powered geysers on triton. *Science*, *250*(4979), 424–429. https://doi.org/10.1126/science.250.4979.424

Knight, C. A. (1987). Slush on lakes. In D. E. Loper (Ed.), *Structure and dynamics of partially solidified systems* (pp. 453–465). Springer. https://doi.org/10.1007/978-94-009-3587-7_22

Landis, G. A. (2007). Observation of frost at the equator of Mars by the opportunity rover. In *38th annual lunar and planetary science conference*.

Langevin, Y., Douté, S., Vincendon, M., Poulet, F., Bibring, J.-P., Gondet, B., et al. (2006). No signature of clear CO_2 ice from the 'cryptic' regions in Mars' south seasonal polar cap. *Nature*, *442*(7104), 790–792. https://doi.org/10.1038/nature05012

Laskar, J., Correia, A., Gastineau, M., Joutel, F., Levrard, B., & Robutel, P. (2004). Long term evolution and chaotic diffusion of the insolation quantities of Mars. *Icarus*, *170*(2), 343–364. https://doi.org/10.1016/j.icarus.2004.04.005

Laskar, J., Levrard, B., & Mustard, J. (2002). Orbital forcing of the Martian polar layered deposits. *Nature*, *419*(6905), 375–377. https://doi.org/10.1038/nature01066

Laskar, J., & Robutel, P. (1993). The chaotic obliquity of the planets. *Nature*, *361*(6413), 608–612. https://doi.org/10.1038/361608a0

Leidenfrost, J. (1966). On the fixation of water in diverse fire. *International Journal of Heat and Mass Transfer*, *9*(11), 1153–1166. https://doi.org/10.1016/0017-9310(66)90111-6

Leighton, R. B., & Murray, B. C. (1966). Behavior of carbon dioxide and other volatiles on Mars. *Science*, *153*(3732), 136–144. https://doi.org/10.1126/science.153.3732.136

Lintott, C., Schawinski, K., Bamford, S., Slosar, A., Land, K., Thomas, D., et al. (2010). Galaxy zoo 1: Data release of morphological classifications for nearly 900 000 galaxies*. *Monthly Notices of the Royal Astronomical Society*, *410*(1), 166–178. https://doi.org/10.1111/j.1365-2966.2010.17432.x

Litvak, M. L., Mitrofanov, I. G., Kozyrev, A. S., Sanin, A. B., Tretyakov, V. I., Boynton, W. V., et al. (2007). Long-term observations of southern winters on Mars: Estimations of column thickness, mass, and volume density of the seasonal CO_2 deposit from HEND/Odyssey data. *Journal of Geophysical Research E: Planets*, *112*(E3), E03S13. https://doi.org/10.1029/2006JE002832

Malin, M., & Edgett, K. (2001). Mars global surveyor Mars orbiter camera: Interplanetary cruise through primary mission. *Journal of Geophysical Research*, *106*(E10), 23429–23570. https://doi.org/10.1029/2000je001455

Mandelbrot, B. (1982). *The fractal geometry of nature*. Times Books.

Mangold, N. (2005). High latitude patterned grounds on Mars: Classification, distribution and climatic control. *Icarus*, *174*(2), 336–359. https://doi.org/10.1016/j.icarus.2004.07.030

Manning, C. V., Bierson, C., Putzig, N. E., & McKay, C. P. (2019). The formation and stability of buried polar CO_2 deposits on Mars. *Icarus*, *317*, 509–517. https://doi.org/10.1016/j.icarus.2018.07.021

Marchant, D. R., Lewis, A. R., Phillips, W. M., Moore, E. J., Souchez, R. A., Denton, G. H., et al. (2002). Formation of patterned ground and sublimation till over Miocene glacier ice in Beacon Valley, southern Victoria Land, Antarctica. *Geological Society of America Bulletin*, *114*(6), 718–730. https://doi.org/10.1130/0016-7606(2002)114<0718:fopgas>2.0.co;2

Martínez, G., Newman, C., De Vicente-Retortillo, A., Fischer, E., Renno, N. O., Richardson, M. I., et al. (2017). The modern near-surface martian climate: A review of in-situ meteorological data from viking to curiosity. *Space Science Reviews*, *212*(1–2), 295–338. https://doi.org/10.1007/s11214-017-0360-x

Massé, M., Conway, S. J., Gargani, J., Patel, M. R., Pasquon, K., McEwen, A., et al. (2016). Transport processes induced by metastable boiling water under Martian surface conditions. *Nature Geoscience*, *9*(6), 425–428. https://doi.org/10.1038/ngeo2706

Matson, D. L., & Brown, R. H. (1989). Solid-state greenhouse and their implications for icy satellites. *Icarus*, *77*(1), 67–81. https://doi.org/10.1016/0019-1035(89)90007-9

Matsuo, K., & Heki, K. (2009). Seasonal and inter-annual changes of volume density of Martian CO_2 snow from time-variable elevation and gravity. *Icarus*, *202*(1), 90–94. https://doi.org/10.1016/j.icarus.2009.02.023

McCord, T. B., Hansen, G. B., Clark, R. N., Martin, P. D., Hibbitts, C. A., Fanale, F. P., et al. (1998). Non-water-ice constituents in the surface material of the icy Galilean satellites from the galileo near-infrared mapping spectrometer investigation. *Journal of Geophysical Research*, *103*(E4), 8603–8626. https://doi.org/10.1029/98JE00788

McEwen, A. S. (2007). Mars reconnaissance orbiter high resolution imaging science experiment, reduced data record. In *MRO-M-HIRISE-3-RDR-V1.1, NASA planetary data system*. https://doi.org/10.17189/1520303

McEwen, A. S., Eliason, E. M., Bergstrom, J. W., Bridges, N. T., Hansen, C. J., Delamere, W. A., et al. (2007). Mars reconnaissance orbiter's high resolution imaging science experiment (HiRISE). *Journal of Geophysical Research: Planets*, *112*(E5), E05S02. https://doi.org/10.1029/2005je002605

Mc Keown, L., Bourke, M., McElwaine, J., Sylvest, M., & Patel, M. (2021). The formation of araneiforms by carbon dioxide venting and vigorous sublimation dynamics under Martian conditions. *Scientific Reports*, *11*(1), 6445. https://doi.org/10.1038/s41598-021-82763-7

Mc Keown, L., Diniega, S., Bourke, M., & Schwamb, M. (2023a). 'Morphometric trends and implications for the Formation of araneiform clusters' (dataset). *Zenodo*. https://doi.org/10.5281/zenodo.7689838

Mc Keown, L., Diniega, S., Bourke, M., & Schwamb, M. (2023b). Morphometric trends and implications for the formation of araneiform clusters. *Earth and Planetary Science Letters*, *607*, 118049. https://doi.org/10.1016/j.epsl.2023.118049

Mc Keown, L., Diniega, S., Dao, J., Hansen, C., Portyankina, G., Piqueux, S., & Aye, K.-M. (2022). A comprehensive map of martian South Polar region araneiform locations and morphological analysis. In *American geophysical union fall meeting*.

Mc Keown, L., Lesage, E., Scully, J., Leonard, E., Pappalardo, R., Potter, M., et al. (2022). Lake stars as an analog for Europa's Manannán crater spider feature. In *AGU fall meeting*.

Mc Keown, L. E., Bourke, M. C., & McElwaine, J. N. (2017). Experiments on sublimating carbon dioxide ice and implications for contemporary surface processes on Mars. *Scientific Reports*, *7*(1), 14181. https://doi.org/10.1038/s41598-017-14132-2

Mellon, M. T. (1997). Small-scale polygonal features on Mars: Seasonal thermal contraction cracks in permafrost. *Journal of Geophysical Research*, *102*(E11), 25617–25628. https://doi.org/10.1029/97JE02582

Mellon, M. T., Feldman, W. C., & Prettyman, T. H. (2004). The presence and stability of ground ice in the southern hemisphere of Mars. *Icarus*, *169*(2), 324–340. https://doi.org/10.1016/j.icarus.2003.10.022

Mellon, M. T., & Jakosky, B. M. (1993). Geographic variations in the thermal and diffusive stability of ground ice on Mars. *Journal of Geophysical Research*, *98*(E2), 3345–3364. https://doi.org/10.1029/92je02355

Mellon, M. T., & Jakosky, B. M. (1995). The distribution and behavior of Martian ground ice during past and present epochs. *Journal of Geophysical Research*, *100*(E6), 11781–11799. https://doi.org/10.1029/95je01027

Mellon, M. T., Jakosky, B. M., & Postawko, S. E. (1997). The distribution and behavior of Martian ground ice during past and present epochs. *Journal of Geophysical Research*, *102*(E8), 19357–19369. https://doi.org/10.1029/97je01346

Mellon, M. T., & Phillips, R. (2001). Recent gullies on Mars and the source of liquid water. *Journal of Geophysical Research*, *106*(E10), 23165–23179. https://doi.org/10.1029/2000je001424

Miall, A. (2013). *Fluvial depositional systems*. Springer.

Michael, G., Platz, T., Kneissl, T., & Schmedemann, N. (2012). Planetary surface dating from crater size, frequency distribution measurements: Spatial randomness and clustering. *Icarus*, *218*(1), 169–177. https://doi.org/10.1016/j.icarus.2011.11.033

Milkovich, S., & Head, J. (2005). North polar cap of Mars: Polar layered deposit characterization and identification of a fundamental climate signal. *Journal of Geophysical Research*, *110*(E1), E01005. https://doi.org/10.1029/2004JE002349

Moore, J. M., Asphaug, E., Belton, M. J., Bierhaus, B., Breneman, H. H., Brooks, S. M., & Williams, K. K. (2001). Impact features on Europa: Results of the Galileo Europa Mission (GEM). *Icarus*, *151*(1), 93–111. https://doi.org/10.1006/icar.2000.6558

Morgan, G. A., Putzig, N. E., Perry, M. R., Sizemore, H. G., Bramson, A. M., Petersen, E. I., et al. (2021). Availability of subsurface water-ice resources in the northern mid-latitudes of Mars. *Nature Astronomy*, *5*(3), 230–236. https://doi.org/10.1038/s41550-020-01290-z

Murray, B. C., Soderblom, L. A., Cutts, J. A., Sharp, R. P., Milton, D. J., & Leighton, R. B. (1972). Geological framework of the South Polar region of Mars. *Icarus*, *17*(2), 328–345. https://doi.org/10.1016/0019-1035(72)90004-8

Nash, C., & Bourke, M. (2015). Southern hemisphere sand furrows: Spatial patterning and implications for the cryo-venting process. In *EGU general assembly conference abstracts* (Vol. 17).

Paige, D. A., Bachman, J. E., & Keegan, K. D. (1994). Thermal and albedo mapping of the polar regions of Mars using viking thermal mapper observations: 1. North Polar region. *Journal of Geophysical Research*, *99*(E12), 25959–25991. https://doi.org/10.1029/93je03428

Paige, D. A., & Keegan, K. D. (1994). Thermal and albedo mapping of the polar regions of Mars using viking thermal mapper observations: 2. South Polar region. *Journal of Geophysical Research*, *99*(E12), 25993–26013. https://doi.org/10.1029/93je03429

Pelletier, J. D., & Turcotte, D. L. (2000). Shapes of river networks and leaves: Are they statistically similar? *Philosophical Transactions of the Royal Society of London. Series B: Biological Sciences*, *355*(1394), 307–311. https://doi.org/10.1098/rstb.2000.0566

Pilorget, C., Edwards, C. S., Ehlmann, B. L., Forget, F., & Millour, E. (2013). Material ejection by the cold jets and temperature evolution of the south seasonal polar cap of Mars from THEMIS/CRISM observations and implications for surface properties. *Journal of Geophysical Research: Planets*, *118*(12), 2520–2536. https://doi.org/10.1002/2013JE004513

Pilorget, C., Forget, F., Millour, E., Vincendon, M., & Madeleine, J. B. (2011). Dark spots and cold jets in the polar regions of Mars: New clues from a thermal model of surface CO_2 ice. *Icarus*, *213*(1), 131–149. https://doi.org/10.1016/j.icarus.2011.01.031

Piqueux, S., Buz, J., Edwards, C. S., Bandfield, J. L., Kleinböhl, A., Kass, D. M., et al. (2019). Widespread shallow water ice on Mars at high latitudesand midlatitudes. *Geophysical Research Letters*, *46*(24), 14290–14298. https://doi.org/10.1029/2019GL083947

Piqueux, S., Byrne, S., Kieffer, H., Titus, T., & Hansen, C. (2015). Enumeration of Mars years and seasons since the beginning of telescopic exploration. *Icarus*, *251*, 332–338. https://doi.org/10.1016/j.icarus.2014.12.014

Piqueux, S., Byrne, S., & Richardson, M. I. (2003). Sublimation of Mars's southern seasonal CO_2 ice cap and the formation of spiders. *Journal of Geophysical Research: Planets*, *108*, 3-1. https://doi.org/10.1029/2002JE002007

Piqueux, S., & Christensen, P. R. (2008a). Deposition of CO_2 and erosion of the martian south perennial cap between 1972 and 2004: Implications for current climate change. *Journal of Geophysical Research E: Planets*, *113*(E2), E02006. https://doi.org/10.1029/2007JE002969

Piqueux, S., & Christensen, P. R. (2008b). North and south subice gas flow and venting of the seasonal caps of Mars: A major geomorphological agent. *Journal of Geophysical Research: Planets*, *113*(E6), E06005. https://doi.org/10.1029/2007je003009

Piqueux, S., Edwards, C. S., & Christensen, P. R. (2008). Distribution of the ices exposed near the south pole of Mars using thermal emission imaging system (themis) temperature measurements. *Journal of Geophysical Research*, *113*(E8), E08014. https://doi.org/10.1029/2007JE003055

Piqueux, S., Kleinböhl, A., Hayne, P. O., Heavens, N. G., Kass, D. M., McCleese, D. J., et al. (2016). Discovery of a widespread low-latitude diurnal CO_2 frost cycle on Mars. *Journal of Geophysical Research: Planets*, *121*(7), 1174–1189. https://doi.org/10.1002/2016je005034

Plaut, J. J., Picardi, G., Safaeinili, A., Ivanov, A. B., Milkovich, S. M., Cicchetti, A., et al. (2007). Subsurface radar sounding of the south polar layered deposits of Mars. *Science*, *316*(5821), 92–95. https://doi.org/10.1126/science.1139672

Portyankina, G., Hansen, C. J., & Aye, K.-M. (2017). Present-day erosion of Martian polar terrain by the seasonal CO_2 jets. *Icarus*, *282*, 93–103. https://doi.org/10.1016/j.icarus.2016.09.007

Portyankina, G., Hansen, C. J., & Aye, K.-M. (2020). How martian araneiforms get their shapes: Morphological analysis and diffusion-limited aggregation model for polar surface erosion. *Icarus*, *342*, 113217. https://doi.org/10.1016/j.icarus.2019.02.032

Portyankina, G., Markiewicz, W. J., Thomas, N., Hansen, C. J., & Milazzo, M. (2010). Hirise observations of gas sublimation-driven activity in Mars' southern polar regions: III. Models of processes involving translucent ice. *Icarus*, *205*(1), 311–320. https://doi.org/10.1016/j.icarus.2009.08.029

Portyankina, G., Merrison, J., Iversen, J. J., Yoldi, Z., Hansen, C. J., Aye, K.-M., et al. (2019). Laboratory investigations of the physical state of CO_2 ice in a simulated Martian environment. *Icarus*, *322*, 210–220. https://doi.org/10.1016/j.icarus.2018.04.021

Portyankina, G., Pommerol, A., Aye, K.-M., Hansen, C. J., & Thomas, N. (2012). Polygonal cracks in the seasonal semi-translucent CO_2 ice layer in martian polar areas. *Journal of Geophysical Research*, *117*(E2), E02006. https://doi.org/10.1029/2011JE003917

Portyankina, G. V. (2005). *Atmosphere-surface vapor exchange and ices in the Martian polar regions* (Doctoral dissertation). Georg August University of Gottingen. Retrieved from https://www.mps.mpg.de/phd/theses/atmosphere-surface-vapor-exchange-and-ices-in-the-martian-polar-regions

Prettyman, T. H., Feldman, W. C., Mellon, M. T., McKinney, G. W., Boynton, W. V., Karunatillake, S., & Tokar, R. L. (2004). Composition and structure of the Martian surface at high southern latitudes from neutron spectroscopy. *Journal of Geophysical Research*, *109*(E5), E05001. https://doi.org/10.1029/2003JE002139

Prieto-Ballesteros, O., Fernández-Remolar, D. C., Rodríguez-Manfredi, J. A., Selsis, F., & Manrubia, S. C. (2006). Spiders: Water-driven erosive structures in the southern hemisphere of Mars. *Astrobiology*, *6*(4), 651–667. https://doi.org/10.1089/ast.2006.6.651

Putzig, N. E., & Mellon, M. T. (2007). Apparent thermal inertia and the surface heterogeneity of Mars. *Icarus*, *191*(1), 68–94. https://doi.org/10.1016/j.icarus.2007.05.013

Putzig, N. E., Mellon, M. T., Herkenhoff, K. E., Phillips, R. J., Davis, B. J., Ewer, K. J., & Bowers, L. M. (2014). Thermal behavior and ice-table depth within the north polar erg of Mars. *Icarus*, *230*, 64–76. https://doi.org/10.1016/j.icarus.2013.07.010

Putzig, N. E., Mellon, M. T., Kretke, K. A., & Arvidson, R. E. (2005). Global thermal inertia and surface properties of Mars from the MGS mapping mission. *Icarus*, *173*(2), 325–341. https://doi.org/10.1016/j.icarus.2004.08.017

Raack, J., Conway, S. J., Herny, C., Balme, M. R., Carpy, S., & Patel, M. R. (2017). Water induced sediment levitation enhances downslope transport on Mars. *Nature Communications*, *8*(1), 1151. https://doi.org/10.1038/s41467-017-01213-z

Saffman, P. G., & Taylor, G. I. (1958). The penetration of a fluid into a porous medium or Hele-Shaw cell containing a more viscous liquid. *Proceedings of the Royal Society of London. Series A. Mathematical and Physical Sciences*, *245*(1242), 312–329. https://doi.org/10.1098/rspa.1958.0085

Schmidt, F., Douté, S., Schmitt, B., Vincendon, M., Bibring, J.-P., Langevin, Y., et al. (2009). Albedo control of seasonal South Polar cap recession on Mars. *Icarus*, *200*(2), 374–394. https://doi.org/10.1016/j.icarus.2008.12.014

Schmidt, F., Schmitt, B., Douté, S., Forget, F., Jian, J.-J., Martin, P., et al. (2010). Sublimation of the Martian CO_2 seasonal south polar cap. *Planetary and Space Science*, *58*(10), 1129–1138. https://doi.org/10.1016/j.pss.2010.03.018

Schorghofer, N., & Edgett, K. S. (2006). Seasonal surface frost at low latitudes on Mars. *Icarus*, *180*(2), 321–334. https://doi.org/10.1016/j.icarus.2005.08.022

Schorghofer, N., & Forget, F. (2012). History and anatomy of subsurface ice on Mars. *Icarus*, *220*(2), 1112–1120. https://doi.org/10.1016/j.icarus.2012.07.003

Schorghofer, N., Williams, J.-P., Martinez-Camacho, J., Paige, D. A., & Siegler, M. A. (2021). Carbon dioxide cold traps on the moon. *Geophysical Research Letters*, *48*(20), e2021GL095533. https://doi.org/10.1029/2021GL095533

Schorgofer, N., Jensen, B., Kudroli, A., & Rothman, D. H. (2004). Spontaneous channelization in permeable ground: Theory, experiment, and observation. *Journal of Fluid Mechanics*, *503*, 357–374. https://doi.org/10.1017/S0022112004007931

Schwamb, M. E., Aye, K.-M., Portyankina, G., Hansen, C. J., Allen, C., Allen, S., et al. (2018). Planet four: Terrains—Discovery of araneiforms outside of the South Polar layered deposits. *Icarus*, *308*, 148–187. https://doi.org/10.1016/j.icarus.2017.06.017

Séjourné, A., Costard, F., Gargani, J., Soare, R., Fedorov, A., & Marmo, C. (2011). Scalloped depressions and small-sized polygons in western utopia planitia, Mars: A new formation hypothesis. *Planetary and Space Science*, *59*(5), 412–422. https://doi.org/10.1016/j.pss.2011.01.007

Séjourné, A., Costard, F., Gargani, J., Soare, R. J., & Marmo, C. (2012). Evidence of an eolian ice-rich and stratified permafrost in Utopia Planitia, Mars. *Planetary and Space Science*, *60*(1), 248–254. https://doi.org/10.1016/j.pss.2011.09.004

Smith, B. A., Soderblom, L. A., Banfield, D., Barnet, c., Basilevsky, A. T., Beebe, R. F., et al. (1989). Voyager 2 at Neptune: Imaging science results. *Science*, *246*(4936), 1422–1449. https://doi.org/10.1126/science.246.4936.1422

Smith, D. E., Zuber, M. T., & Neumann, G. A. (2001). Seasonal variations of snow depth on Mars. *Science*, *294*(5549), 2141–2146. https://doi.org/10.1126/science.1066556

Smith, I. B., Schlegel, N. J., Larour, E., Isola, I., Buhler, P. B., Putzig, N. E., & Greve, R. (2022). Carbon dioxide ice glaciers at the South Pole of Mars. *Journal of Geophysical Research: Planets*, *127*(4), e07193. https://doi.org/10.1029/2022JE007193

Smith, P. H., Tamppari, L. K., Arvidson, R. E., Bass, D., Blaney, D., Boynton, W. V., et al. (2009). H_2O at the phoenix landing site. *Science*, *325*(5936), 58–61. https://doi.org/10.1126/science.1172339

Soare, R., Conway, S., Williams, J.-P., Philippe, M., Mc Keown, L., Godin, E., & Hawkswell, J. (2021). Possible ice-wedge polygonisation in utopia planitia, Mars and its latitudinal gradient of distribution. *Icarus*, *358*, 114208. https://doi.org/10.1016/j.icarus.2020.114208

Soderblom, L. A., Kieffer, S. W., Becker, T. L., Brown, R. H., Cook, A. F., Hansen, C. J., et al. (1990). Triton's geyser-like plumes: Discovery and basic characterization. *Science*, *250*(4979), 410–415. https://doi.org/10.1126/science.250.4979.410

Steinbrügge, G., Voigt, J. R., Wolfenbarger, N. S., Hamilton, C. W., Soderlund, K. M., Young, D. A., et al. (2020). Brine migration and impact-induced cryovolcanism on Europa. *Geophysical Research Letters*, *47*(21), e2020GL090797. https://doi.org/10.1029/2020GL090797

Strahler, A. (1952). Hypsometric (area-altitude) analysis of erosoional topography. *GSA Bulletin*, *63*(11), 1117. https://doi.org/10.1130/0016-7606(1952)63[1117:haaoet]2.0.co;2

Sutton, S. S., Chojnacki, M., McEwen, A. S., Kirk, R. L., Dundas, C. M., Schaefer, E. I., et al. (2022). Revealing active Mars with HiRISE digital terrain models. *Remote Sensing*, *14*(10), 2403. https://doi.org/10.3390/rs14102403

Sylvest, M. E., Conway, S. J., Patel, M. R., Dixon, J. C., & Barnes, A. (2016). Mass wasting triggered by seasonal CO_2 sublimation under Martian atmospheric conditions: Laboratory experiments. *Geophysical Research Letters*, *43*(24), 12. https://doi.org/10.1002/2016gl071022

Sylvest, M. E., Dixon, J., Conway, S., Patel, M., McElwaine, J., Hagermann, A., & Barnes, A. (2018). *CO_2 sublimation in Martian gullies: Laboratory experiments at varied slope angle and regolith grain sizes* (p. 467). Geological Society, London, Special Publications. https://doi.org/10.1144/SP467.11

Tanaka, K., Skinner, J., Dohm, J., Irwin, R., Kolb, E., Fortezzo, C., et al. (2014). *Geologic map of Mars*. U.S. Geological Survey Scientific Investigations. https://doi.org/10.3133/sim3292

Thomas, N., Hansen, C. J., Portyankina, G., & Russell, P. S. (2010). HiRISE observations of gas sublimation-driven activity in Mars's southern polar regions: II. Surficial deposits and their origins. *Icarus*, *205*(1), 296–310. https://doi.org/10.1016/j.icarus.2009.05.030

Thomas, N., Portyankina, G., Hansen, C. J., & Pommerol, A. (2011a). HiRISE observations of gas sublimation-driven activity in Mars's southern polar regions: IV. Fluid dynamics models of CO_2 jets. *Icarus*, *212*(1), 66–85. https://doi.org/10.1016/j.icarus.2010.12.016

Thomas, N., Portyankina, G., Hansen, C. J., & Pommerol, A. (2011b). Sub-surface CO_2 gas flow in Mars' polar regions: Gas transport under constant production rate conditions. *Geophysical Research Letters*, *38*(8), GL046797. https://doi.org/10.1029/2011GL046797

Thomas, P., Squyres, S., Herkenhoff, K. E., Murray, B., & Howard, A. (1992). Polar deposits on Mars. In *Mars* (pp. 767–795).

Thomas, P. C., Malin, M. C., Edgett, K. S., Carr, M. H., Hartmann, W. K., Ingersoll, A. P., et al. (2000). North-south geological differences between the residual polar caps on Mars. *Nature*, *404*(6774), 161–164. https://doi.org/10.1038/35004528

Tillman, J., Johnson, N., Guttorp, P., & Percival, D. (1993). The Martian annual atmospheric pressure cycle: Years without great dust storms. *Journal of Geophysical Research*, *98*(E6), 10963–10971. https://doi.org/10.1029/93je01084

Titus, T. N., Calvin, W. H., Kieffer, H., Langevin, Y., & Prettyman, T. H. (2008). Martian polar processes. In J. Bell (Ed.), *The Martian surface: Composition, mineralogy, and physical properties*. Cambridge University Press.

Titus, T. N., Kieffer, H., & Christensen, P. (2003). Exposed water ice discovered near the south pole of Mars. *Science*, *299*(5609), 1048–1051. https://doi.org/10.1126/science.1080497

Titus, T. N., Williams, K. E., & Cushing, G. E. (2020). Conceptual model for the removal of cold-trapped H_2O ice on the Mars northern seasonal springtime polar cap. *Geophysical Research Letters*, *47*(15), e2020GL087387. https://doi.org/10.1029/2020GL087387

Tsai, V. C., & Wettlaufer, J. S. (2007). Star patterns on lake ice. *Physical Review E*, *75*(6), 066105. https://doi.org/10.1103/PhysRevE.75.066105

Turcotte, D., Pelletier, J., & Newman, W. (1998). Networks with side branching in biology. *Journal of Theoretical Biology*, *193*(4), 577–592. https://doi.org/10.1006/jtbi.1998.0723

Vasavada, A. R., Williams, J.-P., Paige, D. A., Herkenhoff, K. E., Bridges, N. T., Greeley, R., et al. (2000). Surface properties of Mars' polar layered deposits and polar landing sites. *Journal of Geophysical Research*, *105*(E3), 6961–6969. https://doi.org/10.1029/1999JE001108

Vincendon, M., Forget, F., & Mustard, J. (2010). Water ice at low to midlatitudes on Mars. *Journal of Geophysical Research*, *115*(E10), E10001. https://doi.org/10.1029/2010JE003584

Vincendon, M., Mustard, J., Forget, F., Kreslavsky, M., Spiga, A., Murchie, S., & Bibring, J.-P. (2010). Near-tropical subsurface ice on Mars. *Geophysical Research Letters*, *37*(1), L01202. https://doi.org/10.1029/2009GL041426

Warren, S. G. (1986). Optical constants of carbon dioxide ice. *Applied Optics*, *25*(16), 2650–2674. https://doi.org/10.1364/AO.25.002650

Westoby, M., Brasington, J., Glasser, N., Hambrey, M., & Reynolds, J. (2012). Structure-from-Motion photogrammetry: A low-cost, effective tool for geoscience applications. *Geomorphology*, *179*, 300–314. https://doi.org/10.1016/j.geomorph.2012.08.021

Widmer, J. M., Diniega, S., Hayne, P. O., Alsaeed, N., & Gary-Bicas, C. E. (2020). MRO high resolution imaging science experiment (HIRISE): Instrument development. In *2020 AGU fall meeting* (p. P033-0010).

Wieczorek, M. A. (2008). Constraints on the composition of the Martian south polar cap from gravity and topography. *Icarus*, *196*(2), 506–517. https://doi.org/10.1016/j.icarus.2007.10.026

Xiao, H., Stark, A., Schmidt, F., Hao, J., Steinbrügge, G., Wagner, N. L., et al. (2022). Spatio-temporal level variations of the martian seasonal north polar cap from co-registration of mola profiles. *Journal of Geophysical Research: Planets*, *127*(10), e2021JE007158. https://doi.org/10.1029/2021JE007158

Xiao, H., Stark, A., Schmidt, F., Hao, J., Su, S., Steinbrügge, G., & Oberst, J. (2022). Spatio-temporal level variations of the martian seasonal South Polar cap from co-registration of MOLA profiles. *Journal of Geophysical Research, Planets*, *127*(7), e2022JE007196. https://doi.org/10.1029/2022JE007196

Zent, A. P., Hecht, M. H., Cobos, D. R., Wood, S. E., Hudson, T. L., Milkovich, S. M., et al. (2010). Initial results from the thermal and electrical conductivity probe (TECP) on phoenix. *Journal of Geophysical Research*, *115*(E3), E00E14. https://doi.org/10.1029/2009JE003420

Zuber, M., Phillips, R., Andrews-Hanna, J., Asmar, S., Konopliv, A., Lemoine, F., et al. (2007). Density of Mars's South Polar layered deposits. *Science*, *317*(5845), 1718–1719. https://doi.org/10.1126/science.1146995

Zurek, R. W., Barnes, J. R., Haberle, R. M., Pollack, J. B., Tillman, J. E., & Leovy, C. B. (1992). Dynamics of the atmosphere of Mars. In M. George (Ed.), *Mars* (pp. 835–933).